A novel interplay between GEFs orchestrates Cdc42 activity during cell polarity and cytokinesis

Brian Hercyk, Julie Rich, and Maitreyi Das*

Department of Biochemistry & Cellular and Molecular Biology, University of Tennessee, Knoxville, TN, USA.

*CORRESPONDING AUTHOR: mdas@utk.edu

ORCID: 0000-0001-9164-0158

415 Ken and Blaire Mossman Building

1311 Cumberland Ave

University of Tennessee

Knoxville, TN, 37996

CONDENSED TITLE: Gef1 and Scd1 crosstalk to attune Cdc42 activity

SUMMARY

Cdc42 is precisely regulated by unknown mechanisms. Hercyk et al. report that the Cdc42 GEFs regulate each other to spatially control Cdc42 activation during polarized growth and cytokinesis. Elucidation of this crosstalk provides an insight into how multiple GEFs regulating the same GTPase play distinct roles during complex processes.

This manuscript is currently available as a preprint at BioRxiv

DOI: https://www.biorxiv.org/content/early/2018/07/07/364786

ABSTRACT

Cdc42 is activated by the GEFs Gef1 and Scd1 in fission yeast. While *gef1* and *scd1* mutants exhibit distinct phenotypes, the mechanism by which this occurs is unclear given that they activate the same GTPase. We report that Gef1 and Scd1 regulate each other to spatially modulate Cdc42 activity during polarized growth and cytokinesis. We find that Gef1 mediates Scd1 localization via the scaffold Scd2. At the division site this enables proper septum formation, and at the new cell end during interphase this enables the transition from monopolar to bipolar growth. Reciprocally, Scd1 restricts Gef1 localization, via actin, at the division site to facilitate cell separation, and to sites of polarized growth during interphase to maintain cell shape. Our findings reveal an elegant regulatory pattern in which Gef1 establishes new sites of Scd1-mediated Cdc42 activity, while Scd1 restricts Gef1 to functional sites. We propose that crosstalk between GEFs is a conserved mechanism that orchestrates Cdc42 activation during multiple processes.

INTRODUCTION

Growth and division are fundamental processes of all cells, and are essential for proper function and proliferation. In most multicellular organisms, these two processes are precisely tuned to control cell shape and function through polarization. Cell polarization relies on the ability of the cytoskeleton to establish unique domains at the cell cortex to govern the local function and activity of specific proteins (Drubin and Nelson, 1996; Nance and Zallen, 2011). The Rho family of small GTPases serve as the primary regulators of cell polarity and movement via actin regulation (Ridley, 2006). Active Rho GTPases bind and activate downstream targets which regulate actin cytoskeleton organization. GTPases are active when GTP-bound and inactive once they hydrolyze GTP to GDP. Guanine nucleotide Exchange Factors (GEFs) activate GTPases by promoting the binding of GTP, while GTPase Activating Proteins (GAPs) inactivate GTPases by promoting GTP hydrolysis (Bos et al., 2007). Unraveling the regulation of these GEFs and GAPs is at the crux of understanding how cell polarity is established, altered, and maintained. One conserved member of the Rho family of small GTPases, Cdc42, is a master regulator of polarized cell growth and membrane trafficking in eukaryotes (Estravis et al., 2012; Estravis et al., 2011; Etienne-Manneville, 2004; Harris and Tepass, 2010; Johnson, 1999). Like other small GTPases, Cdc42 acts as a binary molecular switch and can respond to and initiate multiple signaling pathways. In most eukaryotes, Cdc42 is regulated by numerous GEFs and GAPs, complicating our understanding of GTPase regulation (Bos et al., 2007). In the fission yeast *Schizosaccharomyces pombe,* Cdc42 is activated by two GEFs, Gef1 and Scd1 (Chang et al., 1994; Coll et al., 2003). The presence of only two Cdc42 GEFs, and the well-documented process of cell polarization in these cells, make fission yeast an excellent model system to understand the mechanistic details of cell shape establishment. Here we report that the two Cdc42 GEFs regulate each other during both cytokinesis and polarized growth. This finding provides new insights into the spatiotemporal regulation of Cdc42 during critical cellular events.

Fission yeast cells are rod shaped and grow in a polarized manner from the two ends. These cells exhibit a unique growth pattern; cells in early G2 phase show monopolar growth, occurring at the old end, that existed in the previous generation. Cells transition to a bipolar growth pattern during late G2 phase through the process of new end take off (NETO), when the cell initiates growth at the new end that was formed during sister cell separation. Due to this simple growth pattern, fission yeast is an excellent model to understand how a cell regulates polarized growth from multiple sites. In fission yeast, active Cdc42 displays anti-correlated oscillations between the two ends (Das et al., 2012). These oscillations arise from both positive and time-delayed negative feedback as well as from competition between the two ends (Das et al., 2012). This oscillatory pattern regulates cell dimensions and promotes bipolar growth in fission yeast. Similar Cdc42 oscillations have been observed in natural killer cells during immunological synapse formation (Carlin et al., 2011) and in budding yeast during bud emergence (Howell et al., 2012). In plant cells, the ROP GTPases show oscillatory behavior during pollen tube growth (Hwang et al., 2005). Furthermore, during migration in animal cells, the GTPases Rho, Rac, and Cdc42 are sequentially activated to enable cell protrusion (Machacek et al., 2009). These observations suggest that oscillatory behavior, which drives cell polarity, may be an intrinsic property of GTPases that is likely conserved in most organisms (Das and Verde, 2013).

Cdc42 undergoes precise spatiotemporal regulation to efficiently promote different cellular processes. In fission yeast, Cdc42 must be activated at the cell ends to promote polarized growth and restricted from the cell sides to maintain cell shape (Das et al., 2012; Das et al., 2009). Cdc42 is also involved in cytokinesis in fission yeast. During cytokinesis, Cdc42 activation is required for proper septum formation, and like in other systems, Cdc42 needs to be subsequently inactivated to promote cell separation (Atkins et al., 2013; Onishi et al., 2013; Wei et al., 2016b). The regulatory mechanisms that allow for these spatiotemporal activation patterns are not well understood. To explain Cdc42 activation during polarized growth, it is important to first understand how Cdc42 regulators function. Gef1 and Scd1 are partially redundant but exhibit unique phenotypes when deleted (Chang et al., 1994; Coll et al., 2003), indicating that they may regulate Cdc42 in distinct, but overlapping, manners. Scd1 oscillates between the two cell ends, much like active Cdc42 (Das et al., 2012), and cells lacking *scd1* appear depolarized (Chang et al., 1994). Scd1 is also required for mating and contributes to Cdc42 dependent exploration of the cell cortex (Bendezu and Martin, 2013). In contrast, *gef1* mutants become narrower and grow in a monopolar, rather than a bipolar, manner (Coll et al., 2003). Furthermore, Cdc42 activity is reduced at the new end in *gef1* mutants (Das et al., 2012). Gef1 shows sparse localization at the cortex, making it difficult to determine whether it oscillates between cell ends (Das et al., 2015). Understanding how two different Cdc42 GEFs yield distinct phenotypes will provide valuable insights into Cdc42 regulation.

Investigations into the behaviors of Gef1 and Scd1 during interphase are complicated since these GEFs overlap at sites of polarized growth. These GEFs also localize to the site of cell division during cytokinesis (Wei et al., 2016b). Cytokinesis, the final step in cell division, involves the formation of an actomyosin ring that constricts, concurrent with cell wall (septum) deposition, to enable membrane ingression and furrow formation (Pollard, 2010). The temporal localization and function of the two GEFs are discernible during cytokinesis since they are recruited to the division site in succession to activate Cdc42. During cytokinesis, Gef1 localizes first to the actomyosin ring to activate Cdc42 and promote ring constriction (Wei et al., 2016b). Next, Scd1 localizes to the ingressing membrane and regulates septum formation (Wei et al., 2016b). The temporal difference between Gef1 and Scd1 localization at the division site allows us to investigate the significance of multiple GEFs in Cdc42 regulation, which is unclear from studies solely of the growing ends.

Using cytokinesis as a paradigm, here we identify a novel crosstalk between the GEFs, Gef1 and Scd1, that regulates Cdc42 activity during multiple cellular programs. We find that Gef1 and Scd1 regulate each other during both cytokinesis and cell polarization. Scd1 is required for proper septum formation. Our data indicate that Gef1 promotes the localization of Scd1 to the division site to promote septum formation. Contrary to previously proposed models, constitutively active Cdc42 is insufficient to rescue Scd1 localization in *gef1* mutants. Instead, we find that Gef1 promotes the localization of the scaffold Scd2 to the division site during cytokinesis, which then recruits Scd1. Next, we show that Scd1 promotes the removal of Gef1 from the division site after completion of ring constriction. Furthermore, actin cables are involved in Gef1 removal from the division site, suggesting that Scd1 promotes Gef1 removal via an actin-mediated process to promote cell separation. We extend these observations to the sites of polarized growth, where we show that Gef1 promotes bipolar Scd1 and Scd2 localization;

indeed, Gef1 is necessary to recruit Scd1 to the non-dominant end to initiate bipolar growth. In turn, Scd1 and actin are necessary to prevent isotropic localization of Gef1 at the cell cortex during interphase, thus maintaining polarity. By this manner of regulation, Cdc42 activation is promoted at the new end of the cell with no prior growth history, but is restricted from random regions. Gef1 recruits Scd1 to new sites to establish Cdc42 activation and in turn, Scd1 restricts Gef1 to functional sites. To the best of our knowledge, such crosstalk has not been reported to function between GEFs of the same GTPase. The interplay between the Cdc42 GEFs operates in the same manner during both cytokinesis and polarized growth, suggesting that this may be a conserved feature of Cdc42 regulation.

RESULTS

Gef1 promotes Scd1 recruitment to the division site

We have reported that Scd1 localizes to the assembled actomyosin ring after Gef1 to activate Cdc42 along the membrane barrier (Wei et al., 2016b). Cdc42 activation at the membrane barrier allows the recruitment of the septum-synthesizing enzyme Bgs1 to this site, and therefore proper septum formation. Previous reports have demonstrated crosstalk between GTPases via modulation of their regulators (Guilluy et al., 2011). While there is no report of GEFs of the same GTPase regulating each other, such an interaction could explain the temporal relationship detected between Gef1 and Scd1 localization at the division site. Since Scd1 arrives at the division site soon after Gef1, we posited that Gef1 may promote Scd1 localization. To test this, we examined whether Scd1 localization to actomyosin rings is Gef1-dependent. Both Gef1 and Scd1 are low-abundance proteins and are not suitable for live cell imaging over time. This complicates the investigation of the temporal localization of these proteins. To overcome this limitation, we used the actomyosin ring as a temporal marker. The actomyosin ring undergoes visibly distinct phases during cytokinesis: assembly, maturation, constriction, and disassembly. We determined the timing of protein localization to the division site by comparing it to the corresponding phase of the actomyosin ring. We have previously reported that ring constriction is delayed in *gef1Δ* mutants (Wei et al., 2016b). To eliminate any bias in protein localization due to this delay, we only analyzed cells in which the rings had initiated constriction. In *gef1Δ* mutants, the number of constricting rings that recruited Scd1-3xGFP decreased to 15% from 96% in *gef1+* (Figure 1A,B, $p<0.0001$). Furthermore, the *gef1Δ* cells that managed to recruit Scd1-3xGFP did not do so as efficiently as *gef1+* cells, given the 15% decrease in Scd1-3xGFP fluorescence intensity at the division site (Figure 1A,C, $p=0.0098$). Thus, Gef1 promotes Scd1 localization to the division site.

To decipher the mechanism by which Gef1 recruits Scd1 to the division site, we tested whether GEF recruitment in fission yeast operates as reported in other systems. GEF recruitment to sites of Cdc42 activity occurs via positive feedback, as reported in budding yeast (Butty et al., 2002; Irazoqui et al., 2003; Kozubowski et al., 2008). In this model, activation of Cdc42 leads to further recruitment of the scaffold Bem1, which then recruits the GEF Cdc24 to the site of activity, thus helping to break symmetry and promote polarized growth. A similar positive feedback may also exist in fission yeast (Das et al., 2012; Das and Verde, 2013). We hypothesized that Gef1-activated Cdc42 acts as a seed for Scd1 recruitment to the division site. To test this, we asked whether constitutive activation of Cdc42 could rescue the Scd1 recruitment defect exhibited by *gef1Δ*. In order for this approach to work, the constitutively active Cdc42 must localize to the division site. Localization of active Cdc42 is visualized via the bio-probe CRIB-3xGFP that specifically binds GTP-Cdc42. Since our previous work reported that Cdc42 activity is reduced at the division site in *gef1Δ* cells (Wei et al., 2016b) we validated this approach by first testing whether constitutively active Cdc42 restores CRIB-3xGFP localization at the division site in *gef1Δ* cells. The constitutively active allele *cdc42G12V* and the bio-marker CRIB-3xGFP were expressed in *gef1+* and *gef1Δ* cells. Mild expression of *cdc42G12V* was sufficient to restore CRIB-3xGFP intensity at the division site to physiological levels in *gef1Δ*, but not in *gef1Δ* with the control vector (Figure 1D,F, $p<0.0001$). Surprisingly, although expression of *cdc42G12V* was able to restore Cdc42 activity at the division site in

gef1Δ cells, it was unable to rescue Scd1-3xGFP localization to the division site in *cdc42G12V gef1Δ* cells (Figure 1E,G). This demonstrates that active Cdc42 alone is not sufficient to recruit Scd1, and that Gef1 is required for this process. Another potential mechanism by which Scd1 could be recruited to the division site is the Cdc42 downstream target kinase Pak1. The Cdc42 ternary complex consists of the GEF Scd1, the scaffold protein Scd2, and the downstream effector Pak1 kinase (Endo et al., 2003). Observations in budding yeast suggest that the PAK kinase may mediate GEF recruitment (Kozubowski et al., 2008). Contrary to this hypothesis, we find that Scd1-3xGFP intensity increases in the *nmt1 switch-off* mutant allele of *pak1*, compared to *pak1*+ cells (Figure S1). These findings support similar observations reported in the hypomorphic temperature-sensitive *pak1* allele, *orb2-34* (Das et al., 2012), and indicate that *pak1* does not facilitate Scd1 recruitment to the site of action.

Gef1 promotes Scd2 localization to the division site, which in turn recruits Scd1

Previous reports have shown that the scaffold Scd2 is required for Scd1 localization to the sites of polarized growth (Kelly and Nurse, 2011). We hypothesized that Gef1 recruits Scd1 to the division site through the scaffold Scd2. If this were true, Scd2-GFP localization to the division site should be Gef1-dependent. Indeed, we find that *gef1Δ* cells displayed a significant decrease in Scd2-GFP containing assembled rings compared to *gef1*+ cells. In *gef1Δ* mutants, the number of rings that recruited Scd2-GFP prior to ring constriction decreased to 8% compared to 88% in *gef1*+, indicating a delay in Scd2 recruitment (Figure 2A,B, $p>0.0001$). Although *gef1Δ* cells were able to recruit Scd2 to the division site once ring constriction began, the fluorescence intensity of Scd2-GFP at the division site was reduced by 61% compared to *gef1*+ cells (Figure 2A,C, $p>0.0001$, Figure S2). Gef1 thus promotes Scd2 localization to the division site.

Since previous work indicates that Scd1 and Scd2 require each other for their localization (Kelly and Nurse, 2011), it is possible that a decrease in Scd2 at the division site observed in *gef1* mutants is due to a decrease in Scd1 at this site. However, contrary to previous findings, we observed that Scd2-GFP localization at the division site is not impaired in *scd1Δ* cells (Figure 2E). In contrast, Scd1-3xGFP localization is completely abolished at the division site in *scd2Δ* cells (Figure 2D). We find that while Scd1 requires Scd2 for its localization to the division site, Scd2 localization is independent of Scd1. Altogether, this reveals that Gef1 promotes Scd2 localization to the division site, which then recruits Scd1. Based on this data, we hypothesized that Gef1, Scd2, and Scd1 sequentially localize to the division site. To test this, we examined the temporal localization of Gef1, Scd2, and Scd1 to the division site. Since these proteins do not lend themselves to extended time lapse imaging, we used the spindle pole bodies as an internal timer. The distance between spindle pole bodies is a well-established temporal marker to determine a cell's cytokinetic stage. The spindle pole body distance increases as mitosis progresses until the cell reaches anaphase B (Nabeshima et al., 1998), at which time the actomyosin ring starts to constrict (Wu et al., 2003). The distance between the two spindle pole bodies can thus act as an internal clock that helps to time the recruitment of other proteins. We acquired numerous still images and calculated the distance between the spindle pole bodies, marked by Sad1-mCherry, during anaphase A or anaphase B. We report the spindle pole body

distance at which Gef1-mNG (monomeric NeonGreen), Scd1-3xGFP, and Scd2-GFP signals are visible at the non-constricting actomyosin ring (Figure 2F). Next, we calculated the mean spindle pole body distance of the first 50th percentile of our data. The protein that localizes earliest to the actomyosin ring during mitosis will display the smallest mean spindle pole body distance. We find that Gef1-mNG localized to the actomyosin ring with a mean spindle pole body distance of 3.2µm, Scd2-GFP with a mean distance of 4.1µm and Scd1-3xGFP with a mean distance of 5.1µm (Figure 2G). This demonstrates that Gef1 is recruited to the actomyosin ring first, followed by Scd2, and finally Scd1, thus supporting our earlier results, which show that Gef1 recruits Scd1 indirectly through Scd2.

Scd1 promotes Gef1 removal from the division site at the end of ring constriction

We have previously shown that prolonged Cdc42 activation at the division site impairs cell separation, as seen in other model systems (Atkins et al., 2013; Onishi et al., 2013; Wei et al., 2016a). This would necessitate the removal of the GEFs from the division site. Gef1 contains a membrane-binding N-BAR domain (Das et al., 2015); accordingly, we find that GEF1-mNG localizes to the membrane behind the Rlc1-tdTomato-marked ring (DATA). Gef1 localization does not expand into the membrane barrier (data). Rather, Scd1-GFP localizes behind Gef1-tdTomato in the membrane barrier (Figure 3A). As the ring constricts, Gef1 constricts with it and is lost from the division site while the ring disassembles (Wei et al., 2016b). At this stage, Scd1 is still localized to the membrane barrier (Figure 3A). Based on these observations we hypothesized that Scd1 facilities Gef1 removal from the division site. To test this, we analyzed Gef1 localization in *scd1Δ* mutants. We observed persistent Gef1 localization in *scd1* mutants after ring constriction. In *scd1Δ* mutants, after completion of ring constriction and disassembly, Gef1 remains at the membrane that was adjacent to the ring (Figure 3B). Among *scd1Δ* cells that had completed constriction, 70% show persistent Gef1-mNG at the newly formed membrane barrier, as confirmed by the absence of Rlc1-tdTomato (Figure 3B,C). Similar Gef1-mNG localization was observed in only 20% of *scd1*+ cells (Figure 3C, $p<0.0001$).

To elucidate the mechanism by which Scd1 mediates Gef1 removal from the membrane barrier after constriction, we analyzed the phenotype of *scd1Δ* mutants. We find that the actin cytoskeleton is disrupted in *scd1Δ* cells, as observed by Alexa Fluor Phalloidin staining. *scd1Δ* cells accumulate actin patches and have fewer and more disorganized actin cables (Figure S3A). We hypothesized that Scd1 facilitates Gef1 removal from the division site via the actin cytoskeleton. To test this, we analyzed Gef1 localization in cells with a disrupted actin cytoskeleton via Latrunculin A (LatA) treatment. In LatA-treated cells that were fully septated following completion of constriction, we observed persistent Gef1 localization at the division site. Gef1-mNG persists on both sides of the septum barrier in 40% of cells treated with LatA, but not in mock DMSO-treated cells (Figure 3D). Cells undergoing ring constriction and septum formation display actin cables as well as Arp2/3-complex-dependent patches at the division site (Coffman et al., 2013; Gachet and Hyams, 2005; Huang et al., 2012; Wang et al., 2016). LatA treatment removes all types of filamentous actin structures (Spector et al., 1983). To determine which actin-mediated process regulates Gef1 removal, we treated cells with CK666 to block only Arp2/3-mediated branched actin filaments (Sun et al., 2011). In these cells, Gef1-mNG

removal was unhindered, as in DMSO-treated control cells, and did not persist at the division site (Figure 3D). This reveals that Gef1 removal at the end of ring constriction is independent of branched actin. We next examined the role of filamentous actin cables in the removal of Gef1 from the membrane barrier. Cdc42 activates the formin For3 to promote actin polymerization and cable formation (Feierbach and Chang, 2001; Martin et al., 2007). Scd1 activates Cdc42, which in turn facilitates For3-mediated actin cable formation, and this may lead to Gef1 removal from the division site. To test this, we investigated Gef1 removal from the membrane barrier in a For3-dependent manner. We find that in *for3Δ*, Gef1-3xYFP lingers at the membrane adjacent to the ring after completion of constriction, just as in *scd1Δ* (Figure 3F). Our data demonstrate that Scd1 regulates the actin cytoskeleton and that Scd1 and actin promote Gef1 removal from the division site. To confirm that Scd1 promotes Gef1 removal via actin, we looked for a functional epistatic relationship between Scd1 and actin. We treated *scd1+* and *scd1Δ* cells expressing Gef1-mNG with LatA or DMSO. We find that in cells treated with DMSO, Gef1-mNG persists in 20% of septated *scd1+* cells and in 63% of septated *scd1Δ* cells. In cells treated with LatA, Gef1-mNG persists in 40% of septated *scd1+* cells and in 61% of septated *scd1Δ* cells (Figure 3E). The extent of Gef1 persistence in *scd1Δ* cells does not increase with the addition of LatA. This indicates that Scd1 is functionally epistatic to actin in the process of Gef1 removal (Figure 3E). Together, these data suggest that Scd1 removes Gef1 from the division site after ring disassembly through an actin-mediated process involving the formin For3.

To determine the significance of Scd1-mediated removal of Gef1 from the division site, we looked at the constitutively localized *gef1S112A* mutant. We confirmed that gef1S112A persists at the division site after ring constriction. In control cells, Gef1-3xYFP is lost from the division site after the completion of ring constriction, indicated by the absence of Cdc15-tdTomato-marked actomyosin ring (Figure S3B). However, Gef1S112A-3xYFP persists at the division site after ring constriction (Figure S3B). Live cell imaging revealed that cell separation is delayed in *gef1S112A* mutants. Cell separation occurred 28 min after ring constriction in *gef1+* cells, but at 34 min in *gef1S112A* mutants (Figure S3C, p=0.009). This further indicates that Scd1-mediated Gef1 removal promotes cell separation.

Gef1 is required for bipolar Scd1 localization

Our data reveal an interesting interplay between the two Cdc42 GEFs in which they regulate each other's localization during cytokinesis. We inquired whether this novel interaction is intrinsic to the regulation of Cdc42 and thus could manifest in other cellular processes. Cdc42 and its GEFs play a supporting role in cytokinesis, but are central players in the regulation of polarized growth. Thus, we asked whether a similar interaction occurs at sites of polarized growth. Fission yeasts display a unique growth pattern in which the cells transition from monopolar to bipolar growth during the cell cycle (Mitchison and Nurse, 1985). Immediately after cell division, monopolar growth occurs with only the old end initiating growth. As the cell cycle progresses, the cells transition to bipolar growth when the new end also initiates growth. Gef1 promotes bipolar growth in fission yeast (Coll et al., 2003; Das et al., 2012). Cells lacking *gef1* show increased monopolarity, with polarized growth only occurring at the old end. Our data show that Gef1 promotes Scd1 recruitment to the division site. Therefore, we hypothesize that

the mechanism for bipolar growth involves Gef1-mediated Scd1 recruitment to the new end. To test this, we analyzed Scd1 localization at the cell ends in *gef1Δ* mutants. Scd1, like active Cdc42, undergoes oscillations between the two competing ends (Das et al., 2012); thus, a cell undergoing bipolar growth does not always display bipolar Scd1 localization. We found that Scd1-3xGFP levels at the old end were comparable in *gef1+* and *gef1Δ* cells (Figure S4). However, *gef1Δ* cells exhibited fewer new ends with Scd1-3xGFP; bipolar Scd1-3xGFP was observed in 30% of interphase *gef1+* cells, but only in 14% of *gef1Δ* cells (Figure 4A,B; p=0.0004).

Previous models suggest that monopolarity in *gef1Δ* cells is due to low levels of active Cdc42 (Das et al., 2012). It is possible that low levels of active Cdc42 resulted in monopolar Scd1 localization in *gef1*Δ cells. To test this, we asked whether expressing constitutively active Cdc42 would restore bipolar Scd1 localization in *gef1*Δ mutants. We first tested whether expression of constitutively active Cdc42 results in bipolar localization of active Cdc42, as indicated by CRIB-3xGFP localization. Low-level expression of *cdc24G12V* was sufficient to restore bipolar CRIB-3xGFP localization in *gef1Δ*, compared to the empty-vector-containing *gef1Δ* mutants (Figure 4B,E; p<0.0001). We observed bipolar CRIB-3xGFP in 75% of *gef1+* cells transformed with the empty vector and in 93% of cells expressing *cdc14G12V*. In *gef1Δ* mutants transformed with the empty vector, we observed bipolar CRIB-3xGFP in only 50% of cells. In contrast, in *gef1Δ* mutants, low levels of *cdc42G12V* expression restored bipolar CRIB-3xGFP in 92% of cells. While *cdc42G12V* expression restored bipolar CRIB-3xGFP in *gef1Δ*, it does not restore bipolar Scd1-3xGFP. We observed bipolar Scd1-3xGFP in 28% of *gef1+* cells transformed with the empty vector, and in 31% of cells expressing *cdc42G12V*. In *gef1Δ* mutants transformed with the empty vector, we observed bipolar Scd1-3xGFP in only 12.5% of cells. Further, in *gef1Δ* mutants expressing low levels of *cdc42G12V*, bipolar Scd1-3xGFP remained in only 12.6% of cells (Figure 4C,E). Thus, expression of *cdc42G12V* failed to restore bipolar Scd1-3xGFP localization to the cell ends in *gef1Δ* mutants, just as it failed to rescue Scd1 localization to the division site (Figure 3C). This demonstrates that Gef1 is required for bipolar Scd1 localization, which does not operate via a simple Cdc42 feedback pathway.

Next, we probed the mechanism by which Gef1 promotes bipolar localization of Scd1 at the cell ends. Since our data indicate that Gef1 recruits Scd1 via the scaffold Scd2 at the division site, we hypothesized that Gef1 promotes bipolar Scd1 localization similarly via Scd2. To test this, we analyzed Scd2 localization at the cell ends in *gef1Δ* mutants. We observed a decrease in bipolar Scd2 in cells lacking *gef1*; 70% of *gef1+* cells displayed bipolar Scd2-GFP localization, but this was reduced to 30% in *gef1Δ* cells (Figure 4A,B, p<0.0001). In support of these findings we also observed that Scd2 is required for Scd1 localization to sites of polarized growth, but Scd2 localization is independent of Scd1 (Figure 4F). In *scd1Δ* mutants, Scd2-GFP signal was observed either at cell ends or ectopically at the cell cortex. In contrast, *scd2Δ* mutants failed to localize Scd1-3xGFP to the cell cortex, forcing its accumulation within the nucleus or cytoplasm (Figure 4F). Based on these data we propose that Gef1 promotes Scd2 localization, which in turn recruits Scd1 to sites of polarized growth.

Gef1 establishes polarized growth at the new end

While *gef1Δ* mutants are mainly monopolar, we find that about 40**%** of interphase cells show bipolar growth (Figure 5B) (Coll et al., 2003; Das et al., 2012; Das et al., 2015). Moreover, we find that about 14% of *gef1Δ* mutants displayed Scd1 localization at the new end (Figure 4A,B). Conversely, constitutively localized *gef1S112A* mutants are precociously bipolar, with the new end initiating growth immediately after cell division (Das et al., 2015). Previous models suggest that monopolarity in *gef1Δ* mutants and bipolarity in *gef1S112A* mutants are due to changes in Gef1-mediated Cdc42 activation at the cell ends (Das et al., 2012; Das et al., 2015). However, we show that Gef1 is required for bipolar Scd1 localization even in cells expressing constitutively active Cdc42. To understand the significance of Gef1-mediated Scd1 localization at the new end, we first investigated the nature of bipolar growth in *gef1Δ* mutants. Fission yeast cells have an old end that existed in the previous generation and a new end that was formed as a result of cell division. The old end initiates growth immediately after completion of division and cell separation. As the cell elongates, it eventually begins to grow at the new end, resulting in bipolar growth (Figure 5A) (Mitchison and Nurse, 1985). The two ends in fission yeast compete for active Cdc42; at first the old end wins this competition (Das et al., 2012). The old end can thus be said to be dominant over the new end in a newborn cell, and always initiates growth first. The new end must overcome the old end's dominance in order to initiate its own growth.

We find that 68% of monopolar *gef1Δ* mutant cells exhibit a growth pattern in which one daughter cell is monopolar and the other daughter cell is prematurely bipolar (Figures 5B and S5). In monopolar *gef1Δ* cells, growth predominantly occurs at the old end, which grew in the previous generation (Figures 5B and S5). In these monopolar cells, the new end frequently fails to grow since it cannot overcome the old end's dominance. The daughter cell that inherits its parent cell's non-growing end typically displays precocious bipolar growth, indicating that these cells do not contain a dominant end. Our data suggest that for a cell end to be dominant it needs to have grown in the previous generation. These results indicate that the new ends of *gef1* cells are not well-equipped to overcome old end dominance. Indeed, we find that in *gef1+* cells, 97% of daughter cells derived from a growing end display a normal growth pattern in which new end take-off occurs only after the old end initiates growth (Figure 5C). In *gef1Δ* cells, only 9% of daughter cells derived from a growing end display the same pattern; instead, 81% of daughter cells derived from a growing end failed to initiate growth at their new end and were thus monopolar (Figure 5C). These data reveal that Gef1 enables the new end to overcome old end dominance to promote bipolar growth.

We hypothesize that Gef1-mediated Scd1 localization enables the new end to overcome old end dominance. This predicts that increased Gef1 levels at the new end will enhance Scd1 localization. Indeed, we find that Scd1 is significantly more bipolar in *gef1S112A* mutants. 53% of *gef1S112A* cells exhibit Scd1-3xGFP localization at both ends, compared to 32% in *gef1+* cells (Figure 5D,E, $p<0.0001$). These findings support the hypothesis that Gef1 overcomes old end dominance by recruiting Scd1 to the new end to establish a nascent growth site.

Scd1 is required to restrict Gef1 localization to the cell ends

Since we find that Scd1 is required for Gef1 removal from the division site, we posit that Scd1 also regulates Gef1 at sites of polarized growth. Cells lacking *scd1* are round, and upon cell cycle arrest, these cells show polarized growth with increased cell width (Chang et al., 1994; Kelly and Nurse, 2011). We asked whether polarity defects in *scd1Δ* mutants arises from aberrant Cdc42 activity due to mislocalized Gef1. To test this, we first analyzed CRIB-3xGFP localization in *scd1Δ* mutants. We find that active Cdc42 appears depolarized in *scd1Δ* mutants during interphase. While CRIB-3xGFP remains restricted to the ends in *scd1+* cells, in *scd1Δ* mutants its localization appears as random patches all over the cortex (Figure 6Bi, ii). Next, we asked whether depolarized CRIB-3xGFP in *scd1*Δ mutants was due to the mislocalization of Gef1. We find that in *scd1+* cells, Gef1-mNG is mostly cytoplasmic and displayed sparse but polarized localization at cell ends (Figure 6Ai). In *scd1Δ* mutants, Gef1-mNG localization at the cortex was prominent when compared to that in *scd1+* cells (Figure 6Aii). Further, Gef1-mNG showed depolarized cortical localization in *scd1Δ* mutants with random patches all over the cortex. This indicates that Scd1 is required to restrict Gef1 localization to the cell ends, thus maintaining polarized growth.

Our findings suggest that, at the division site, Scd1 regulates the actin cytoskeleton (Figure S3A), which in turn promotes Gef1 removal (Figure 3B,C). Therefore, we asked whether actin plays a similar role in Scd1-mediated regulation of Gef1 localization at sites of polarized growth. To test this, we first disrupted the actin cytoskeleton by LatA treatment in cells expressing Gef1-mNG. Gef1-mNG localizes to the ends of control cells treated with DMSO. Upon LatA treatment, Gef1-mNG localizes to ectopic patches at the cortex (Figure 6Av). Next, we analyzed whether Gef1-mNG localization in LatA-treated cells was functionally epistatic to Gef1-mNG localization in *scd1Δ* mutants. Indeed, we find that Gef1-mNG mislocalization was similar in *scd1*Δ mutants treated with either DMSO or LatA and appeared as broad ectopic patches along the cortex (Figure 6Aiv, vi). To determine if ectopic cortical Gef1, arising from LatA-treatment, results in ectopic Cdc42 activation, we analyzed CRIB-3xGFP localization in these cells. We find that in cells treated with LatA, CRIB-3xGFP localizes randomly to the cortex, signifying ectopic Cdc42 activation (Figure 6Bvii), similar to previous reports (Mutavchiev et al., 2016). In mock DMSO-treated control cells, CRIB-3xGFP forms caps at the growing ends (Figure 6Biv). If ectopic Cdc42 activation in LatA-treated cells occurs due to ectopic Gef1 localization, then loss of *gef1* should restore polarized Cdc42 activation in these cells. Indeed, CRIB-3xGFP remains polarized upon LatA treatment in *gef1Δ* mutants (Figure 6Bix). Further, CRIB-3xGFP localization appears as diffuse cortical patches in *scd1Δ* mutants treated with either DMSO or LatA (Figure 6Bv, viii). This indicates that Scd1 is functionally epistatic to actin in the removal of Gef1 from the cell cortex. Together, these data demonstrate that Scd1 is required to prevent ectopic Gef1 localization and Cdc42 activation to maintain proper cell shape and this is likely mediated by the actin cytoskeleton.

DISCUSSION

While Cdc42 is a major regulator of polarized cell growth, its regulation is not well understood, largely due to the presence of multiple activators and inhibitors that often function in a redundant manner. In fission yeast, Cdc42 is activated by only two GEFs, Gef1 and Scd1 (Chang et al., 1994; Coll et al., 2003). While these GEFs are partially redundant (Coll et al., 2003; Hirota et al., 2003), they display distinct phenotypes and it is unclear why the cell requires two Cdc42 GEFs. We have recently shown that Gef1 and Scd1 localize sequentially to the division site to activate Cdc42 during cytokinesis (Wei et al., 2016b). Here we take advantage of the temporal difference between Gef1 and Scd1 localization at the division site to determine the significance of these two GEFs in Cdc42 regulation. We uncover a novel interplay between the Cdc42 GEFs that functions in both cytokinesis and polarized cell growth (Figure 7A). Given the conserved nature of Cdc42 and its regulators, we posit that this interplay between the GEFs is a common feature of Cdc42 regulation.

Crosstalk between Gef1 and Scd1 during cytokinesis

We have previously reported that Gef1 recruitment precedes Scd1 localization to the division site (Wei et al., 2016b). Given that Scd1 appears to be the primary Cdc42 GEF, we asked whether the role of Gef1 is to recruit Scd1. Indeed, we report that Scd1 localizes to the division site in a Gef1-dependent manner (Figure 7B). We report that Scd1 is recruited by its scaffold Scd2, which is in turn recruited by Gef1 (Figure 7A,B). Furthermore, we show that while Scd1 localization is dependent on Scd2, the reciprocal is not true. Unlike the cell ends, the division site has no prior history of Cdc42 activation or Scd1 localization. It is possible that the division site, lacking a prior history of Cdc42 activation, requires Gef1 to recruit Scd1 to this nascent site.

Mis-regulation of Cdc42 has been reported to result in cytokinesis failure in many organisms. Specifically, failure to inactivate Cdc42 leads to failed cell abscission in budding yeast and HeLa cells, and prevents cellularization in *Drosophila* embryos (Atkins et al., 2013; Crawford et al., 1998; Dutartre et al., 1996; Onishi et al., 2013). The mechanism by which Cdc42 is inactivated prior to cell abscission is unclear. Gef1 localization to the division site is lost after ring constriction (Wei et al., 2016b). Here, we show that Scd1 promotes the clearance of Gef1 from the division site after ring disassembly (Figure 7A). This suggests that Scd1 ensures that Gef1 does not persist at the division site in the final stages of cytokinesis, preventing inappropriate Cdc42 activation. Our data also show that Gef1 removal depends on the presence of actin cables and the formin For3 (Figure 7A). Actin cytoskeleton organization is primarily regulated by Cdc42 (Sit and Manser, 2011). We find that ***scd1Δ*** mutants show depolarized actin cables and patches likely due to mis-regulation of Cdc42. We posit that Scd1-dependent actin cytoskeleton organization promotes Gef1 removal from the division site after ring disassembly. Together, our data demonstrate an elegant regulatory pattern in which Gef1-mediated Scd1 recruitment to the division site promotes septum formation, and Scd1-mediated Gef1 removal to promote cell separation.

Gef1 and Scd1 cooperate to drive polarized cell growth

Since we observed that Gef1 recruits Scd1 to the division site, we addressed whether this crosstalk also occurs at sites of polarized growth. Indeed, we find that Gef1 is necessary for bipolar localization of Scd1 and Scd2. Cells lacking *gef1* are mostly monopolar, with polarized growth occurring only at the old end (Coll et al., 2003; Das et al., 2012). This demonstrates that Gef1 promotes bipolar growth by recruiting Scd1 and Scd2. We report that while constitutively active Cdc42 itself is bipolar, it is insufficient to restore bipolar localization of Scd1 in *gef1* mutants. This suggests that active Cdc42 alone does not feed into a positive feedback pathway to promote bipolar Scd1 localization. Our findings highlight a requirement for Gef1 in this process. The new end is a nascent growth site that must activate Cdc42 in the absence of pre-established cues to initiate bipolar growth. Analysis of the growth pattern of *gef1Δ* mutants indicates that new ends frequently fail to overcome old end dominance, resulting in monopolar growth in these cells. Bipolar growth in *gef1Δ* mutants is typically observed in cells that do not contain a dominant old end. Taken together, our findings show that Gef1 allows the new end to overcome old end dominance through Scd1 recruitment and Cdc42 activation, leading to bipolar growth (Figure 7C). *gef1S112A* mutants (Das et al., 2015) and constitutively active Cdc42 mutants, both display bipolar growth. However, only *gef1S112A* mutants display bipolar Scd1 localization in which both the old and the new end recruit Scd1 and initiate growth almost immediately after completion of division. This provides further evidence that Gef1 promotes Scd1 recruitment to initiate bipolar growth.

In fission yeast, Scd1 is the primary GEF that promotes polarized growth (Chang et al., 1994). We find that cells lacking *scd1* are depolarized due to ectopic Cdc42 activation, as a result of mislocalized Gef1. In the presence of *scd1*, Gef1 shows sparse localization and is restricted to the cell ends. Cells lacking *scd1*, fail to restrict Gef1 localization to the ends (Figure 7C). We find that Gef1 is mislocalized in the absence of the actin cytoskeleton, leading to ectopic Cdc42 activation. Furthermore, ectopic Cdc42 activation in LatA-treated cells is abolished in *gef1Δ* mutants. This demonstrates that the ectopic Cdc42 activation observed in LatA-treated cells is Gef1-dependent. Since *scd1* mutants display defects in actin organization, we posit that Scd1 promotes polarized Gef1 localization via the actin cytoskeleton. In support of this hypothesis, we find that Scd1 is epistatic to actin in the process of Gef1 removal. A recent report shows that ectopic Cdc42 activation in LatA-treated cells depends on the stress-activated MAP kinase Sty1 (Mutavchiev et al., 2016). Fission yeast cells treated with LatA did not display ectopic Cdc42 activation in the absence of *sty1*. It is possible that in the absence of actin the cells elicit a stress response, leading to Sty1 activation that results in the mislocalization of Gef1. Further analysis is necessary to test this hypothesis.

Multiple GEFs combinatorially regulate Cdc42 during complex processes

Here we report an interesting interplay between Gef1 and Scd1, in which Gef1 promotes Scd1-mediated Cdc42 activation while Scd1 prevents inappropriate Gef1 mediated Cdc42 activation. Thus, Gef1 and Scd1 crosstalk establishes and maintains polarized growth. Polarized cell growth requires symmetry breaking, and several models have indicated a need for Cdc42 positive feedback loops in this process (Bendezu et al., 2015; Irazoqui et al., 2003; Kozubowski et al., 2008; Slaughter et al., 2009a; Slaughter et al., 2009b). In one model, Cdc42 activation via actin organization and membrane trafficking amplifies its own localization to the polarized tip

(Wedlich-Soldner et al., 2004). Another model, based on studies in fission yeast, describe a positive feedback where active Cdc42 captures inactive molecules to amplify the signal (Bendezu et al., 2015). Elegant experiments in budding yeast demonstrate that local activation of Cdc42 establishes positive feedback through the recruitment of additional GEFs to amplify the conversion of Cdc42-GDP to Cdc42-GTP (Butty et al., 2002; Kozubowski et al., 2008). We expected Gef1-mediated recruitment of Scd1 to function via local activation of Cdc42, which would recruit Scd1 through the establishment of positive feedback. We report that active Cdc42 is not sufficient to recruit Scd1 in the absence of Gef1. While it has been proposed that Cdc42 establishes positive feedback through the formation of the ternary complex consisting of the Cdc42 effector PAK (p21-activated kinases) and its associated scaffold protein (Scd2 or Bem1) (Butty et al., 2002; Kozubowski et al., 2008), studies in *S. pombe* and *S. cerevisiae* suggest that Pak1 kinase activity antagonizes either the Cdc42 scaffold or the GEF, rather than establishing a positive feedback (Das et al., 2012; Gulli et al., 2000; Kuo et al., 2014; Rapali et al., 2017). In support of this antagonistic role of Pak1, we find that more Scd1 accumulates at cell ends and at the division site in the *pak1* switch-off mutant. This indicates that Pak1 does not drive positive feedback, but rather serves to limit the level of Cdc42 activation. Our findings that active Cdc42 failed to recruit Scd1 in the absence of *gef1* do not agree with current models of Cdc42-mediated positive feedback. This may be due, in part, to the fact that most of these models are based on studies in budding yeast. An alternate hypothesis that can explain our observations is that Cdc42 needs to cycle between an active and an inactive form, to establish a positive feedback and recruit the GEFs. Cycling between the active and inactive forms of Cdc42 was precluded from our studies through the use of the constitutively active *cdc42G12V* allele. Thus, the mechanisms that generate feedbacks critical to many biological processes merit further investigation.

Cdc42 activation undergoes an oscillatory pattern at the cell ends that promotes bipolarity. Current models to explain these oscillations indicate the presence of positive feedback, time-delayed negative feedback, and competition between the two ends for active Cdc42. Since Scd1 is the Cdc42 GEF that establishes polarized growth, we posit that Scd1 activates Cdc42 through positive feedback at the dominant old end. Dominance at the old end ensures that Scd1 localization is mainly restricted to this end at the expense of the new end. A previous model suggests that as the cell reaches a certain size, the GEFs reach a threshold level that allows the new end to overcome old end dominance to initiate growth and promote bipolarity (Das et al., 2012). Threshold GEF levels alone cannot explain our findings since *gef1S112A* cells display bipolar growth at a smaller cell size. While an increase in Scd1 levels may promote bipolarity, our data reveal that Gef1-mediated Scd1 recruitment may be a major factor in establishing bipolar growth.

Our finding that active Cdc42 alone does not promote localization of Scd1 to nascent sites may provide an advantage to the cell. A caveat of a positive feedback model driven solely by active Cdc42 is that any stochastic activation of Cdc42 at the cell cortex may generate random Scd1-mediated growth sites. Our data indicate that active Cdc42 is not sufficient to localize Scd1 to additional sites of growth. Instead, in a cell containing a dominant Cdc42 activation site, Gef1 must help recruit Scd1 to the new end to allow bipolar growth (Figure 7C). Given that Gef1 promotes Scd1-mediated polarized growth at the new end, it is conceivable that Gef1 itself is tightly regulated to prevent random Cdc42 activation. Indeed, Gef1 shows sparse localization to the cell ends and is mainly cytoplasmic (Das et al., 2015). The NDR kinase Orb6 prevents ectopic Gef1 localization via 14-3-3-mediated sequestration to the cytoplasm (Das et al., 2015;

Das et al., 2009). Here we show that while Gef1 promotes Scd1 recruitment to a nascent site, Scd1 itself restricts Gef1 localization to the cell ends to precisely activate Cdc42 (Figure 7C). Together our findings describe an elegant system in which the two Cdc42 GEFs regulate each other to ensure proper cell polarization.

Significance of GEF coordination in other systems

The mammalian homolog of Gef1 is the Dynamin binding protein, TUBA (Das et al., 2015). During lumen formation in MDCK cells, TUBA facilitates apical membrane polarization (Bryant et al., 2010; Qin et al., 2010). This suggests that polarization of new sites may be a conserved feature of these GEFs. In budding yeast, CDC24 is required for polarization during bud emergence and is essential for viability (Sloat et al., 1981; Sloat and Pringle, 1978), unlike Scd1 in fission yeast. Budding yeast also has a second GEF Bud3, which establishes a proper bud site (Kang et al., 2014). During G1 in budding yeast, bud emergence occurs via biphasic Cdc42 activation by the two GEFs: Bud3 helps select the bud site (Kang et al., 2014), and Cdc24 allows polarization (Sloat et al., 1981; Sloat and Pringle, 1978). This is analogous to new end growth in fission yeast, which requires Gef1-dependent recruitment of Scd1 for robust Cdc42 activation. It would be interesting to test whether crosstalk also exists between Bud3 and Cdc24.

The Rho family of GTPases includes Rho, Rac, and Cdc42. In certain mammalian cells, Cdc42 and Rac1 appear to activate cell growth in a biphasic manner (de Beco et al., 2018; Yang et al., 2016). For example, during motility, the GTPases, Rho, Rac, and Cdc42, regulate the actin cytoskeleton (Heasman and Ridley, 2008; Machacek et al., 2009). During cell migration, these GTPases form bands or ‘zones’ in the leading and trailing regions of the cell (Ridley, 2015). Their spatial separation is mediated by the organization of their GEFs and GAPs, as well as by regulatory signaling between these GTPases (Guilluy et al., 2011). Cdc42 and Rho are mutually antagonistic, explaining how such zones of GTPase activity can be established and maintained (Guilluy et al., 2011; Kutys and Yamada, 2014; Warner and Longmore, 2009). Similarly, Cdc42 can refine Rac activity (Guilluy et al., 2011). Cdc42 and Rac are activated by similar pathways and share the same effectors. Several recent experiments demonstrate that, during cell migration, reorganization of the actin cytoskeleton occurs in a biphasic manner, in which Cdc42 activation at new sites sets the direction, while robust Rac activation determines the speed (de Beco et al., 2018; Yang et al., 2016). Unlike most eukaryotes, the genome of *S. pombe* does not contain a Rac GTPase. We speculate that the two Cdc42 GEFs of *S. pombe* allow it to fulfill the roles of both Cdc42 and Rac. Gef1 sets the direction of growth by establishing growth at a new site, while Scd1 promotes efficient growth through robust Cdc42 activation at the growth sites. In conclusion, we propose that the crosstalk between the Cdc42 GEFs themselves is an intrinsic property of small GTPases and is necessary for fine-tuning their activity.

MATERIALS AND METHODS

Strains and cell culture

The *S. pombe* strains used in this study are listed in Supplemental Table S1. All strains are isogenic to the original strain PN567. Cells were cultured in yeast extract (YE) medium and grown exponentially at 25°C, unless specified otherwise. Standard techniques were used for genetic manipulation and analysis (Moreno et al., 1991). Cells were grown exponentially for at least 3 rounds of eight generations each before imaging.

Microscopy

Cells were imaged at room temperature (23–25°C) with an Olympus IX83 microscope equipped with a VTHawk two-dimensional array laser scanning confocal microscopy system (Visitech International, Sunderland, UK), electron-multiplying charge-coupled device digital camera (Hamamatsu, Hamamatsu City, Japan), and 100×/numerical aperture 1.49 UAPO lens (Olympus, Tokyo, Japan). Images were acquired with MetaMorph (Molecular Devices, Sunnyvale, CA) and analyzed by ImageJ (National Institutes of Health, Bethesda, MD).

Actin staining

The actin cytoskeleton was stained by Alexa Fluor Phalloidin as described here (Das et al., 2009; Pelham and Chang, 2001). Briefly, exponentially growing cells were fixed with 3.5% formaldehyde for 10 minutes at room temperature. the fixed cells were washed with PM buffer (35 mM KPO4, pH 6.8, 0.5 mM MgSO4) permeabilized with 1% triton X-100 and stained with Alexa Fluor Phalloidin (Molecular Probes) for 30 minutes.

Analysis of growth pattern

The growth pattern of *gef1+* and *gef1Δ* cells was observed by live imaging of cells through multiple generations. Cells were placed in 3.5-mm glass-bottom culture dishes (MatTek, Ashland, MA) and overlaid with YE medium plus 1% agar, and 100μM ascorbic acid to minimize photo-toxicity to the cell. A bright-field image was acquired every minute for 12 hours. Birth scars were used to distinguish between, as well as to measure, old end and new end growth.

Construction of fluorescently tagged Gef1 fusion proteins

The forward primer 5'-CCCGGGAACCCTCGCAGCTAAAGA-3' with a 5' BamHI site and the reverse primer 5'-GGATCCGTGTTTACCAAAGTTATGTAAGAC-3' with a 5' XmaI site were used to amplify a 3kb DNA fragment containing *gef1*, the 5' UTR, and the endogenous promoter. The fragment was then digested with BamHI and XmaI and ligated into the BamHI-XmaI site of pKS392 pFA6-tdTomato-kanMX and pKG6507 pFA6-mNeonGreen-kanMX. Constructs were linearized by digestion with XbaI and transformed into the *gef1* locus in *gef1Δ* cells.

Expression of constitutively active Cdc42

pjk148-nmt41x-leu1^{+} or *pjk148-nmt41x:cdc42G12V-leu1*$^{+}$ were linearized with NdeI and integrated into the *leu1-32* locus in *gef1+* and *gef1Δ* cells expressing either CRIB-3xGFP or Scd1-3xGFP. The empty vector *pjk148-nmt41x-leu1*$^{+}$ was used as control. Cells were grown in YE to promote minimal expression of *cdc42G12V*.

Latrunculin A treatment

Cells in YE were incubated at room temperature with 10μM Latrunculin A (Millipore-Sigma) dissolved in dimethyl sulfoxide (DMSO) for 40 min prior to imaging. Control cells were treated with 1% DMSO and incubated for 40 min.

CK666 treatment

Cells in YE were incubated at room temperature with 100μM CK666 (Sigma-Aldrich) dissolved in dimethyl sulfoxide (DMSO) for 5 min prior to imaging. Control cells were treated with 1% DMSO and incubated for 5 min.

Analysis of fluorescent intensity

Mutants expressing fluorescent proteins were grown to OD 0.5 and imaged on slides. Cells in slides were imaged for no more than 3 minutes to prevent any stress response as previously described (Das et al., 2015). Depending on the mutant and the fluorophore, 16-28 Z-planes were collected at a z-interval of 0.4μm for either or both the 488nm and 561nm channels. The respective controls were grown and imaged in an identical manner. ImageJ was used to generate sum projections from the z-series, and to measure the fluorescence intensity of a selected region (actomyosin ring, or growth cap at cell tip). The background fluorescence in a cell-free region of the image was subtracted to generate the normalized intensity. Mean normalized intensity was calculated for each image from all (n>5) measurable cells within each field. A Student's two-tailed t-test, assuming unequal variance, was used to determine significance through comparison of each strain's mean normalized intensities.

ACKNOWLEDGEMENTS

We thank J. Bembenek and T. Burch-Smith for critical review of our manuscript; K. Gould for supplying plasmids; and M. Balasubramanian, and S. Martin for providing strains. This work was supported by a grant from the National Science Foundation (1616495). J.R. was supported by NIH IMSD (R25GM086761) and is currently supported by an NSF GRFP (1452154).

AUTHOR CONTRIBUTIONS

B.H. and M.D. designed experiments. B.H. and J.R. performed experiments and analyzed data. B.H., J.R., and M.D. wrote the manuscript.

DECLARATION OF INTEREST

The authors do not have any financial and non-financial competing interests.

REFERENCES

Atkins, B.D., S. Yoshida, K. Saito, C.F. Wu, D.J. Lew, and D. Pellman. 2013. Inhibition of Cdc42 during mitotic exit is required for cytokinesis. *J Cell Biol*. 202:231-240.

Bendezu, F.O., and S.G. Martin. 2013. Cdc42 explores the cell periphery for mate selection in fission yeast. *Curr Biol*. 23:42-47.

Bendezu, F.O., V. Vincenzetti, D. Vavylonis, R. Wyss, H. Vogel, and S.G. Martin. 2015. Spontaneous Cdc42 polarization independent of GDI-mediated extraction and actin-based trafficking. *PLoS Biol*. 13:e1002097.

Bos, J.L., H. Rehmann, and A. Wittinghofer. 2007. GEFs and GAPs: critical elements in the control of small G proteins. *Cell*. 129:865-877.

Bryant, D.M., A. Datta, A.E. Rodriguez-Fraticelli, J. Peranen, F. Martin-Belmonte, and K.E. Mostov. 2010. A molecular network for de novo generation of the apical surface and lumen. *Nat Cell Biol*.

Butty, A.C., N. Perrinjaquet, A. Petit, M. Jaquenoud, J.E. Segall, K. Hofmann, C. Zwahlen, and M. Peter. 2002. A positive feedback loop stabilizes the guanine-nucleotide exchange factor Cdc24 at sites of polarization. *EMBO J*. 21:1565-1576.

Carlin, L.M., R. Evans, H. Milewicz, L. Fernandes, D.R. Matthews, M. Perani, J. Levitt, M.D. Keppler, J. Monypenny, T. Coolen, P.R. Barber, B. Vojnovic, K. Suhling, F. Fraternali, S. Ameer-Beg, P.J. Parker, N.S. Thomas, and T. Ng. 2011. A targeted siRNA screen identifies regulators of Cdc42 activity at the natural killer cell immunological synapse. *Sci Signal*. 4:ra81.

Chang, E.C., M. Barr, Y. Wang, V. Jung, H.P. Xu, and M.H. Wigler. 1994. Cooperative interaction of S. pombe proteins required for mating and morphogenesis. *Cell*. 79:131-141.

Coffman, V.C., J.A. Sees, D.R. Kovar, and J.Q. Wu. 2013. The formins Cdc12 and For3 cooperate during contractile ring assembly in cytokinesis. *J Cell Biol*. 203:101-114.

Coll, P.M., Y. Trillo, A. Ametzazurra, and P. Perez. 2003. Gef1p, a new guanine nucleotide exchange factor for Cdc42p, regulates polarity in Schizosaccharomyces pombe. *Molecular biology of the cell*. 14:313-323.

Crawford, J.M., N. Harden, T. Leung, L. Lim, and D.P. Kiehart. 1998. Cellularization in Drosophila melanogaster is disrupted by the inhibition of rho activity and the activation of Cdc42 function. *Dev Biol*. 204:151-164.

Das, M., T. Drake, D.J. Wiley, P. Buchwald, D. Vavylonis, and F. Verde. 2012. Oscillatory Dynamics of Cdc42 GTPase in the Control of Polarized Growth. *Science*.

Das, M., I. Nunez, M. Rodriguez, D.J. Wiley, J. Rodriguez, A. Sarkeshik, J.R. Yates, 3rd, P. Buchwald, and F. Verde. 2015. Phosphorylation-dependent inhibition of Cdc42 GEF Gef1 by 14-3-3 protein Rad24 spatially regulates Cdc42 GTPase activity and oscillatory dynamics during cell morphogenesis. *Mol Biol Cell*.

Das, M., and F. Verde. 2013. Role of Cdc42 dynamics in the control of fission yeast cell polarization. *Biochem Soc Trans*. 41:1745-1749.

Das, M., D.J. Wiley, X. Chen, K. Shah, and F. Verde. 2009. The conserved NDR kinase Orb6 controls polarized cell growth by spatial regulation of the small GTPase Cdc42. *Curr Biol*. 19:1314-1319.

de Beco, S., K. Vaidziulyte, J. Manzi, F. Dalier, F. Di Frederico, G. Cornilleau, M. Dahan, and M. Coppey. 2018. Optogenetic dissection of Rac1 and Cdc42 gradient shaping. *bioRxiv*.

Drubin, D.G., and W.J. Nelson. 1996. Origins of cell polarity. *Cell*. 84:335-344.

Dutartre, H., J. Davoust, J.P. Gorvel, and P. Chavrier. 1996. Cytokinesis arrest and redistribution of actin-cytoskeleton regulatory components in cells expressing the Rho GTPase CDC42Hs. *J Cell Sci*. 109 (Pt 2):367-377.

Endo, M., M. Shirouzu, and S. Yokoyama. 2003. The Cdc42 binding and scaffolding activities of the fission yeast adaptor protein Scd2. *J Biol Chem*. 278:843-852.

Estravis, M., S. Rincon, and P. Perez. 2012. Cdc42 regulation of polarized traffic in fission yeast. *Commun Integr Biol*. 5:370-373.

Estravis, M., S.A. Rincon, B. Santos, and P. Perez. 2011. Cdc42 regulates multiple membrane traffic events in fission yeast. *Traffic*. 12:1744-1758.

Etienne-Manneville, S. 2004. Cdc42--the centre of polarity. *Journal of cell science*. 117:1291-1300.

Feierbach, B., and F. Chang. 2001. Roles of the fission yeast formin for3p in cell polarity, actin cable formation and symmetric cell division. *Current biology : CB*. 11:1656-1665.

Gachet, Y., and J.S. Hyams. 2005. Endocytosis in fission yeast is spatially associated with the actin cytoskeleton during polarised cell growth and cytokinesis. *J Cell Sci*. 118:4231-4242.

Guilluy, C., R. Garcia-Mata, and K. Burridge. 2011. Rho protein crosstalk: another social network? *Trends Cell Biol*. 21:718-726.

Gulli, M.P., M. Jaquenoud, Y. Shimada, G. Niederhauser, P. Wiget, and M. Peter. 2000. Phosphorylation of the Cdc42 exchange factor Cdc24 by the PAK-like kinase Cla4 may regulate polarized growth in yeast. *Mol Cell*. 6:1155-1167.

Harris, K.P., and U. Tepass. 2010. Cdc42 and vesicle trafficking in polarized cells. *Traffic*. 11:1272-1279.

Heasman, S.J., and A.J. Ridley. 2008. Mammalian Rho GTPases: new insights into their functions from in vivo studies. *Nat Rev Mol Cell Biol*. 9:690-701.

Hirota, K., K. Tanaka, K. Ohta, and M. Yamamoto. 2003. Gef1p and Scd1p, the Two GDP-GTP exchange factors for Cdc42p, form a ring structure that shrinks during cytokinesis in Schizosaccharomyces pombe. *Mol Biol Cell*. 14:3617-3627.

Howell, A.S., M. Jin, C.F. Wu, T.R. Zyla, T.C. Elston, and D.J. Lew. 2012. Negative feedback enhances robustness in the yeast polarity establishment circuit. *Cell*. 149:322-333.

Huang, J., Y. Huang, H. Yu, D. Subramanian, A. Padmanabhan, R. Thadani, Y. Tao, X. Tang, R. Wedlich-Soldner, and M.K. Balasubramanian. 2012. Nonmedially assembled F-actin cables incorporate into the actomyosin ring in fission yeast. *J Cell Biol*. 199:831-847.

Hwang, J.U., Y. Gu, Y.J. Lee, and Z. Yang. 2005. Oscillatory ROP GTPase activation leads the oscillatory polarized growth of pollen tubes. *Mol Biol Cell*. 16:5385-5399.

Irazoqui, J.E., A.S. Gladfelter, and D.J. Lew. 2003. Scaffold-mediated symmetry breaking by Cdc42p. *Nat Cell Biol*. 5:1062-1070.

Johnson, D.I. 1999. Cdc42: An essential Rho-type GTPase controlling eukaryotic cell polarity. *Microbiology and molecular biology reviews : MMBR*. 63:54-105.

Kang, P.J., M.E. Lee, and H.O. Park. 2014. Bud3 activates Cdc42 to establish a proper growth site in budding yeast. *J Cell Biol*. 206:19-28.

Kelly, F.D., and P. Nurse. 2011. Spatial control of Cdc42 activation determines cell width in fission yeast. *Mol Biol Cell*. 22:3801-3811.

Kozubowski, L., K. Saito, J.M. Johnson, A.S. Howell, T.R. Zyla, and D.J. Lew. 2008. Symmetry-breaking polarization driven by a Cdc42p GEF-PAK complex. *Current biology : CB*. 18:1719-1726.

Kuo, C.C., N.S. Savage, H. Chen, C.F. Wu, T.R. Zyla, and D.J. Lew. 2014. Inhibitory GEF phosphorylation provides negative feedback in the yeast polarity circuit. *Curr Biol*. 24:753-759.

Kutys, M.L., and K.M. Yamada. 2014. An extracellular-matrix-specific GEF-GAP interaction regulates Rho GTPase crosstalk for 3D collagen migration. *Nat Cell Biol*. 16:909-917.

Machacek, M., L. Hodgson, C. Welch, H. Elliott, O. Pertz, P. Nalbant, A. Abell, G.L. Johnson, K.M. Hahn, and G. Danuser. 2009. Coordination of Rho GTPase activities during cell protrusion. *Nature*. 461:99-103.

Martin, S.G., S.A. Rincon, R. Basu, P. Perez, and F. Chang. 2007. Regulation of the formin for3p by cdc42p and bud6p. *Molecular biology of the cell*. 18:4155-4167.

Mitchison, J.M., and P. Nurse. 1985. Growth in cell length in the fission yeast Schizosaccharomyces pombe. *Journal of cell science*. 75:357-376.

Moreno, S., A. Klar, and P. Nurse. 1991. Molecular genetic analysis of fission yeast Schizosaccharomyces pombe. *Methods in enzymology*. 194:795-823.

Mutavchiev, D.R., M. Leda, and K.E. Sawin. 2016. Remodeling of the Fission Yeast Cdc42 Cell-Polarity Module via the Sty1 p38 Stress-Activated Protein Kinase Pathway. *Curr Biol*. 26:2921-2928.

Nabeshima, K., T. Nakagawa, A.F. Straight, A. Murray, Y. Chikashige, Y.M. Yamashita, Y. Hiraoka, and M. Yanagida. 1998. Dynamics of centromeres during metaphase-anaphase transition in fission yeast: Dis1 is implicated in force balance in metaphase bipolar spindle. *Mol Biol Cell*. 9:3211-3225.

Nance, J., and J.A. Zallen. 2011. Elaborating polarity: PAR proteins and the cytoskeleton. *Development*. 138:799-809.

Onishi, M., N. Ko, R. Nishihama, and J.R. Pringle. 2013. Distinct roles of Rho1, Cdc42, and Cyk3 in septum formation and abscission during yeast cytokinesis. *J Cell Biol*. 202:311-329.

Pelham, R.J., and F. Chang. 2001. Role of actin polymerization and actin cables in actin-patch movement in Schizosaccharomyces pombe. *Nature cell biology*. 3:235-244.

Pollard, T.D. 2010. Mechanics of cytokinesis in eukaryotes. *Curr Opin Cell Biol*. 22:50-56.

Qin, Y., W.H. Meisen, Y. Hao, and I.G. Macara. 2010. Tuba, a Cdc42 GEF, is required for polarized spindle orientation during epithelial cyst formation. *J Cell Biol*. 189:661-669.

Rapali, P., R. Mitteau, C. Braun, A. Massoni-Laporte, C. Unlu, L. Bataille, F.S. Arramon, S.P. Gygi, and D. McCusker. 2017. Scaffold-mediated gating of Cdc42 signalling flux. *Elife*. 6.

Ridley, A.J. 2006. Rho GTPases and actin dynamics in membrane protrusions and vesicle trafficking. *Trends Cell Biol*. 16:522-529.

Ridley, A.J. 2015. Rho GTPase signalling in cell migration. *Curr Opin Cell Biol*. 36:103-112.

Sit, S.T., and E. Manser. 2011. Rho GTPases and their role in organizing the actin cytoskeleton. *J Cell Sci*. 124:679-683.

Slaughter, B.D., A. Das, J.W. Schwartz, B. Rubinstein, and R. Li. 2009a. Dual modes of cdc42 recycling fine-tune polarized morphogenesis. *Developmental cell*. 17:823-835.

Slaughter, B.D., S.E. Smith, and R. Li. 2009b. Symmetry breaking in the life cycle of the budding yeast. *Cold Spring Harbor Perspect Biol*. 1:a003384.

Sloat, B.F., A. Adams, and J.R. Pringle. 1981. Roles of the CDC24 gene product in cellular morphogenesis during the Saccharomyces cerevisiae cell cycle. *J Cell Biol*. 89:395-405.

Sloat, B.F., and J.R. Pringle. 1978. A mutant of yeast defective in cellular morphogenesis. *Science*. 200:1171-1173.

Spector, I., N.R. Shochet, Y. Kashman, and A. Groweiss. 1983. Latrunculins: novel marine toxins that disrupt microfilament organization in cultured cells. *Science*. 219:493-495.

Sun, S.C., Z.B. Wang, Y.N. Xu, S.E. Lee, X.S. Cui, and N.H. Kim. 2011. Arp2/3 complex regulates asymmetric division and cytokinesis in mouse oocytes. *PLoS One*. 6:e18392.

Wang, N., I.J. Lee, G. Rask, and J.Q. Wu. 2016. Roles of the TRAPP-II Complex and the Exocyst in Membrane Deposition during Fission Yeast Cytokinesis. *PLoS Biol*. 14:e1002437.

Warner, S.J., and G.D. Longmore. 2009. Cdc42 antagonizes Rho1 activity at adherens junctions to limit epithelial cell apical tension. *J Cell Biol*. 187:119-133.

Wedlich-Soldner, R., S.C. Wai, T. Schmidt, and R. Li. 2004. Robust cell polarity is a dynamic state established by coupling transport and GTPase signaling. *J Cell Biol*. 166:889-900.

Wei, B., B.S. Hercyk, N. Mattson, A. Mohammadi, J. Rich, E. DeBruyne, M.M. Clark, and M. Das. 2016a. Unique Spatiotemporal Activation Pattern of Cdc42 by Gef1 and Scd1 Promotes Different Events during Cytokinesis. *Molecular biology of the cell*.

Wei, B., B.S. Hercyk, N. Mattson, A. Mohammadi, J. Rich, E. DeBruyne, M.M. Clark, and M. Das. 2016b. Unique spatiotemporal activation pattern of Cdc42 by Gef1 and Scd1 promotes different events during cytokinesis. *Mol Biol Cell*. 27:1235-1245.

Wu, J.Q., J.R. Kuhn, D.R. Kovar, and T.D. Pollard. 2003. Spatial and temporal pathway for assembly and constriction of the contractile ring in fission yeast cytokinesis. *Dev Cell*. 5:723-734.

Yang, H.W., S.R. Collins, and T. Meyer. 2016. Locally excitable Cdc42 signals steer cells during chemotaxis. *Nat Cell Biol*. 18:191-201.

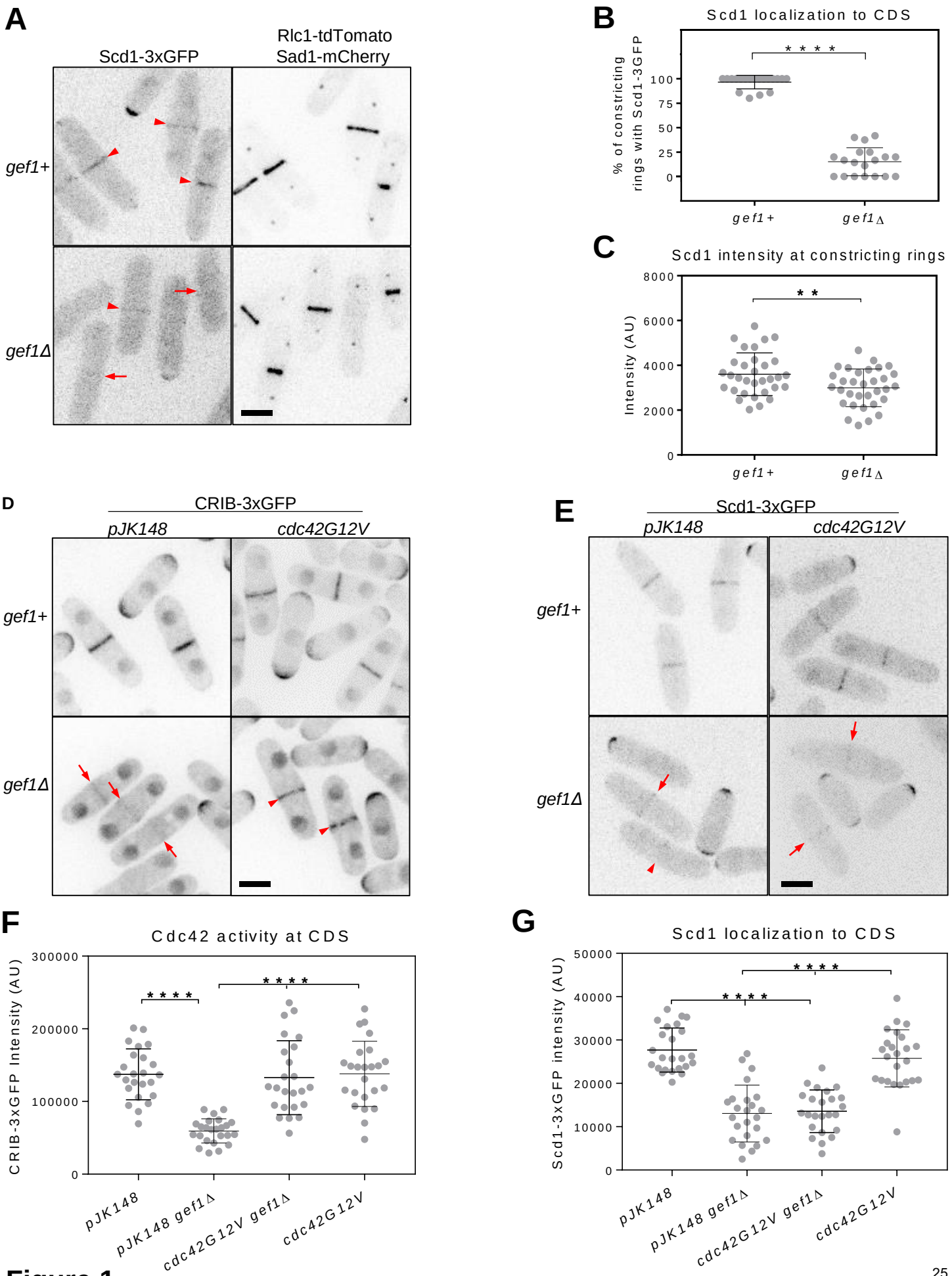
A
Scd1-3xGFP
Rlc1-tdTomato
Sad1-mCherry
gef1+
gef1Δ
B
Scd1 localization to CDS
% of constricting rings with Scd1-3GFP
100
75
50
25
0
* * * *
gef1+
gef1Δ
C
Scd1 intensity at constricting rings
Intensity (AU)
8000
6000
4000
2000
0
* *
gef1+
gef1Δ
D
CRIB-3xGFP
pJK148
cdc42G12V
gef1+
gef1Δ
E
Scd1-3xGFP
pJK148
cdc42G12V
gef1+
gef1Δ
F
Cdc42 activity at CDS
CRIB-3xGFP Intensity (AU)
300000
200000
100000
0
* * * *
* * * *
pJK148
pJK148 gef1Δ
cdc42G12V gef1Δ
cdc42G12V
G
Scd1 localization to CDS
Scd1-3xGFP intensity (AU)
50000
40000
30000
20000
10000
0
* * * *
* * * *
pJK148
pJK148 gef1Δ
cdc42G12V gef1Δ
cdc42G12V

Figure 1

Figure 1: Gef1 promotes Scd1 localization to the division site. (A) Scd1-3xGFP localization in *gef1+* and *gef1Δ* cells expressing the ring and SPB markers Rlc1-tdTomato and Sad1-mCherry respectively. Arrowheads label cells with Scd1-3xGFP localized to the division site, while arrows mark cells with constricting rings that lack Scd1-3xGFP at the division site. **(B and C)** Quantification of Scd1-3xGFP localization and intensity in the indicated genotypes (**, $p<0.01$). **(D)** CRIB-3xGFP, the active Cdc42 sensor, intensity at the division site in *gef1+* and *gef1Δ* cells transformed with the control vector *pJK148* or *cdc42G12V*. Arrows label cells with reduced Cdc42 activity at the division site and arrowheads indicate cells with increased Cdc42 activity. **(E)** Scd1-3xGFP localization at the division site in *gef1+* and *gef1Δ* cells transformed with the control vector *pJK148* or *cdc42G12V*. Arrows label cells with reduced Scd1-3xGFP at the division site. **(F and G)** Quantifications of *cdc42G12V*-mediated Cdc42 activity and Scd1 localization at the division site in the indicated genotypes (****, $p<0.0001$). All data points are plotted in each graph, with black bars on top of data points that show the mean and standard deviation for each genotype. All images are inverted max projections. Scale bars = 5µm. Cell Division Site, CDS.

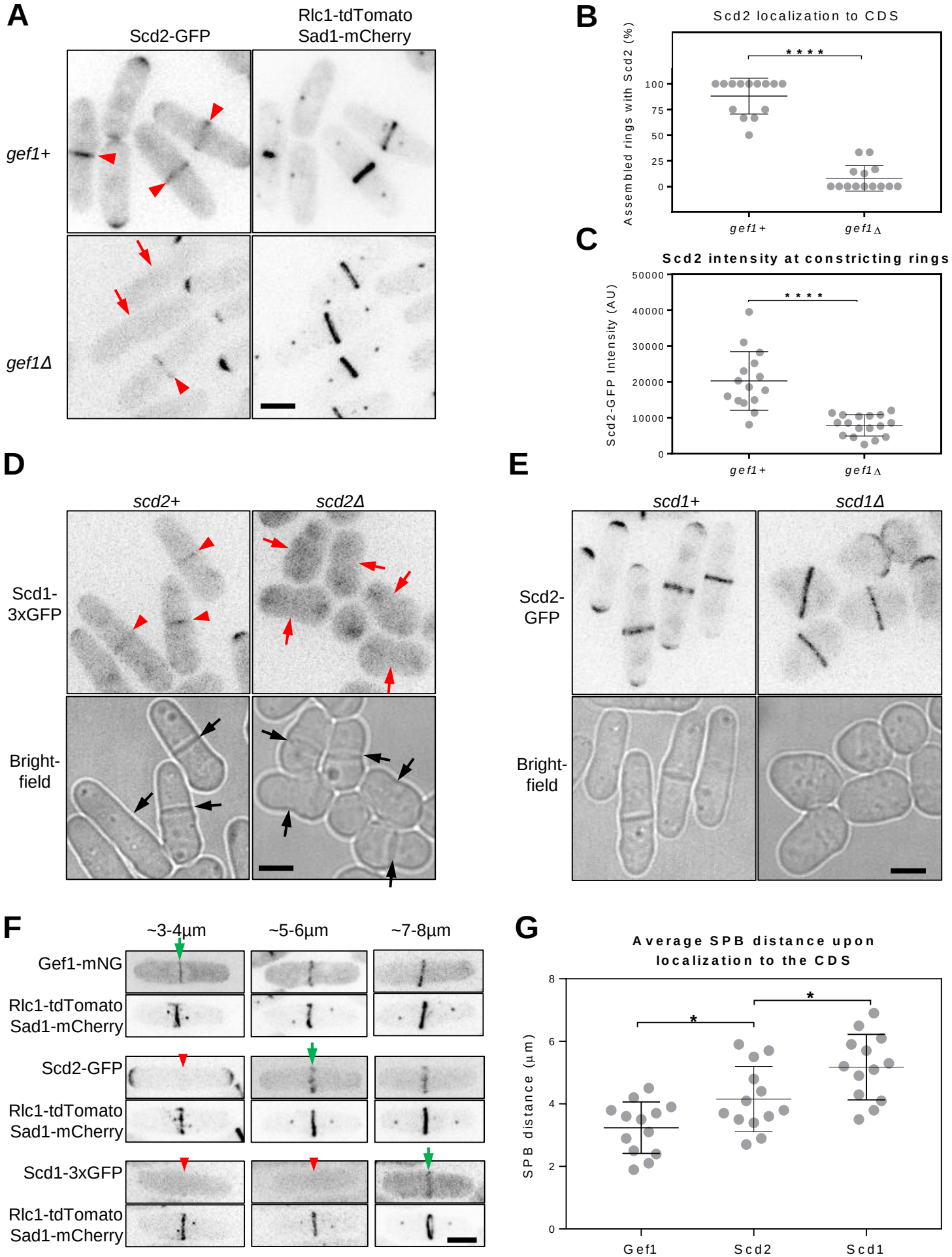
A
Scd2-GFP
Rlc1-tdTomato
Sad1-mCherry
gef1+
gef1Δ
B
Scd2 localization to CDS
Assembled rings with Scd2 (%)
100
75
50
25
0
****
gef1+
gef1Δ
C
Scd2 intensity at constricting rings
Scd2-GFP Intensity (AU)
50000
40000
30000
20000
10000
0
****
gef1+
gef1Δ
D
scd2+
scd2Δ
Scd1-3xGFP
Bright-field
E
scd1+
scd1Δ
Scd2-GFP
Bright-field
F
~3-4µm
~5-6µm
~7-8µm
Gef1-mNG
Rlc1-tdTomato
Sad1-mCherry
Scd2-GFP
Rlc1-tdTomato
Sad1-mCherry
Scd1-3xGFP
Rlc1-tdTomato
Sad1-mCherry
G
Average SPB distance upon localization to the CDS
SPB distance (µm)
8
6
4
2
0
*
*
Gef1
Scd2
Scd1

Figure 2

Figure 2: Gef1 promotes Scd1 localization to the division site via recruitment of Scd2. (A) Scd2 localization in *gef1+* and *gef1Δ* cells expressing the ring and SPB markers Rlc1-tdTomato and Sad1-mCherry. Arrowheads label cells with Scd2-GFP localized constricting rings, while arrows mark cells with assembled rings that lack Scd2-GFP at the division site. **(B and C)** Quantification of Scd2-GFP localization and intensity in the indicated genotypes (****, $p<0.0001$). **(D)** Scd1-3xGFP localization in *scd2+* and *scd2Δ* cells. Division site marked by black arrows in the bright field images. Scd1-3xGFP localization to the division site indicated by red arrowheads. Red arrows show absence of Scd1-3xGFP at the division site. **(E)** Scd2-GFP localization to the division site in *scd1+* and *scd1Δ* cells. **(F)** Representative images showing the localizations of Gef1-mNG, Scd2-GFP, and Scd1-3GFP (top panels) as a function of spindle pole body distance (bottom panels). The range of SPB distance is listed for each column. Green arrows indicate the earliest time point at which signal is visible. Red arrowheads indicate time points prior to localization. **(G)** Quantification of Gef1, Scd2, and Scd1 localization to the division site in a temporal manner, showing the means of the distance between spindle poles of the first 50th percentile of early anaphase cells at which signal first appears (*, $p<0.05$). All data points are plotted in each graph, with black bars on top of data points that show the mean and standard deviation for each genotype. All images are inverted max projections with the exception of bright field. Scale bars = 5µm. Cell Division Site, CDS.

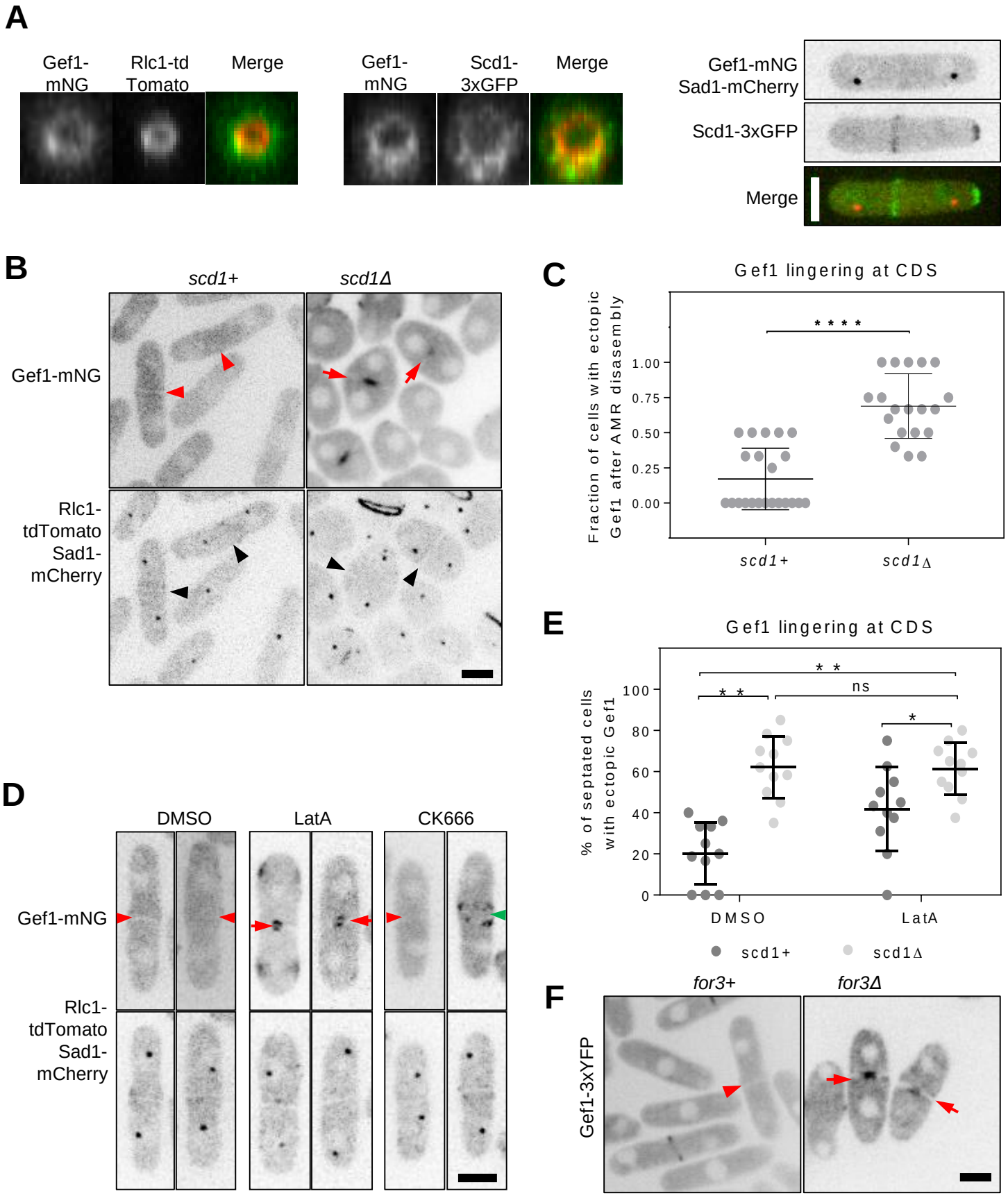
A
Gef1-mNG
Rlc1-td Tomato
Merge
Gef1-mNG
Scd1-3xGFP
Merge
Gef1-mNG
Sad1-mCherry
Scd1-3xGFP
Merge
B
scd1+
scd1Δ
Gef1-mNG
Rlc1-tdTomato
Sad1-mCherry
C
Gef1 lingering at CDS
Fraction of cells with ectopic Gef1 after AMR disassembly
1.00
0.75
0.50
0.25
0.00
* * * *
scd1+
scd1Δ
D
DMSO
LatA
CK666
Gef1-mNG
Rlc1-tdTomato
Sad1-mCherry
E
Gef1 lingering at CDS
% of septated cells with ectopic Gef1
100
80
60
40
20
0
* *
ns
*
DMSO
LatA
scd1+
scd1Δ
F
for3+
for3Δ
Gef1-3xYFP

Figure 3

Figure 3: Scd1 and actin promote Gef1 removal from the division site after ring constriction. (A) 3D reconstructions of the division site of cells expressing Gef1-mNG and Rlc1-tdTomato (left panel), and Gef1-mNG and Scd1-3xGFP (middle panel). Gef1-mNG and Scd1-3xGFP localization to the division site after ring disassembly in cells expressing Sad1-mCherry (right panel). **(B)** Gef1-mNG localization to the division site after ring disassembly in *scd1+* and *scd1Δ* cells expressing the ring and SPB markers Rlc1-tdTomato and Sad1-mCherry. Black arrowheads mark the membrane barrier in cells post-ring disassembly. Red arrowheads mark cells post-ring disassembly that lack Gef1-mNG at the membrane barrier. Red arrows mark cells with Gef1-mNG localized to the membrane barrier post-ring assembly. **(C)** Quantification of Gef1 lingering at the division site in *scd1+* and *scd1Δ* cells (****, $p<0.0001$). **(D)** Gef1-mNG localization in septated cells expressing the ring and SPB markers Rlc1-tdTomato and Sad1-mCherry, treated with either DMSO, 10µM LatA, or 100µM CK666. Red arrowheads mark cells post-ring disassembly that lack Gef1-mNG at the membrane barrier. Red arrows indicate cells with Gef1-mNG localized to the membrane barrier post-ring assembly. Green arrowheads indicate cells with Gef1-mNG localized to the cortex orthogonal to the membrane barrier. **(E)** Quantification of Gef1 lingering at the division site in septated *scd1+* and *scd1Δ* cells treated with 10µM LatA or DMSO (*, $p<0.05$. **,$p<0.01$). **(F)** Gef1-3xYFP localization in *for3+* and *for3Δ* cells. Red arrowheads mark cells post-ring disassembly that lack Gef1-3xYFP at the membrane barrier. Red arrows mark cells with Gef1-3xYFP localized to the membrane barrier post-ring assembly. All data points are plotted in each graph, with black bars on top of data points that show the mean and standard deviation for each genotype. All images are inverted max projections unless specified. Scale bars = 5µm. Cell Division Site, CDS.

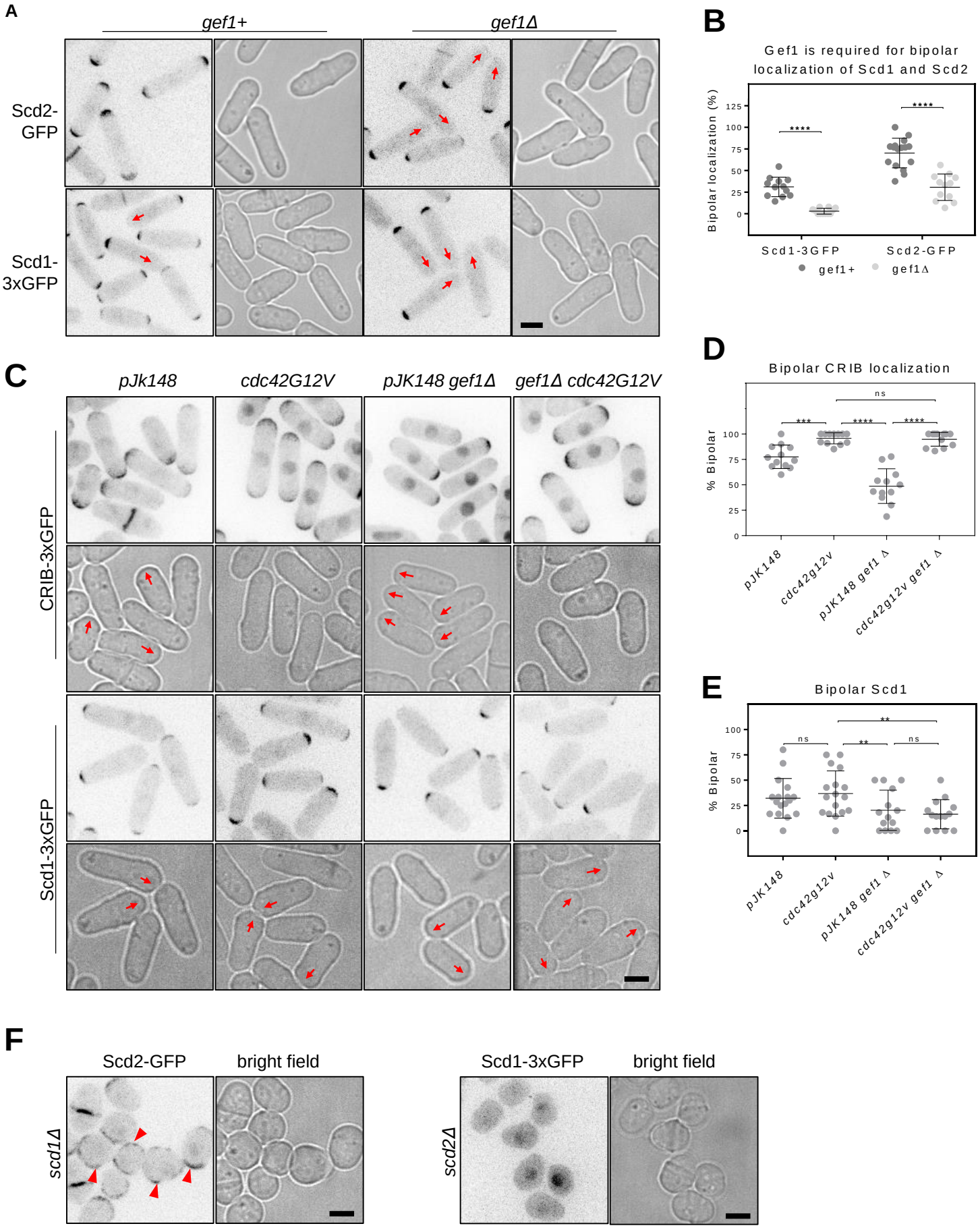
A
gef1+
gef1Δ
Scd2-GFP
Scd1-3xGFP
B
Gef1 is required for bipolar localization of Scd1 and Scd2
Bipolar localization (%)
125
100
75
50
25
0
****
****
Scd1-3GFP
Scd2-GFP
gef1+
gef1Δ
C
pJk148
cdc42G12V
pJK148 gef1Δ
gef1Δ cdc42G12V
CRIB-3xGFP
Scd1-3xGFP
D
Bipolar CRIB localization
% Bipolar
ns
***
****
****
pJK148
cdc42g12v
pJK148 gef1 Δ
cdc42g12v gef1 Δ
E
Bipolar Scd1
% Bipolar
**
ns
**
ns
pJK148
cdc42g12v
pJK148 gef1 Δ
cdc42g12v gef1 Δ
F
Scd2-GFP
bright field
scd1Δ
Scd1-3xGFP
bright field
scd2Δ

Figure 4

Figure 4: Gef1 promotes Scd1 localization to the new end. (A) Scd2-GFP (top panel) and Scd1-3xGFP (bottom panel) localization to the sites of polarized growth in *gef1+* and *gef1Δ* cells. Red arrows indicate the new ends of monopolar cells that do not recruit Scd2-GFP or Scd1-3xGFP. **(B)** Quantifications of bipolar Scd1-3xGFP and Scd2-GFP localization in the indicated genotypes (***, $p<0.001$, ****, $p<0.0001$). **(C)** CRIB-3xGFP and Scd1-3xGFP localization at cell tips, and restoration of bipolar growth in *gef1+* and *gef1Δ* cells transformed with the control vector *pJK148* or *cdc42G12V*. Red arrows indicate the new end of monopolar cells. **(D and E)** Quantification of the percent of cells that exhibit bipolar CRIB-3xGFP and Scd1-3xGFP localization at cell tips in the indicated genotypes (**, $p<0.01$). **(F)** Scd2-GFP and Scd1-3xGFP localization to the cortex in *scd1Δ* and *scd2Δ* cells, respectively. Red arrows indicate cells with Scd2-GFP localized tot the cell cortex. All data points are plotted in each graph, with black bars on top of data points that show the mean and standard deviation for each genotype. All images are inverted max projections with the exception of bright field unless specified. Scale bars = 5µm.

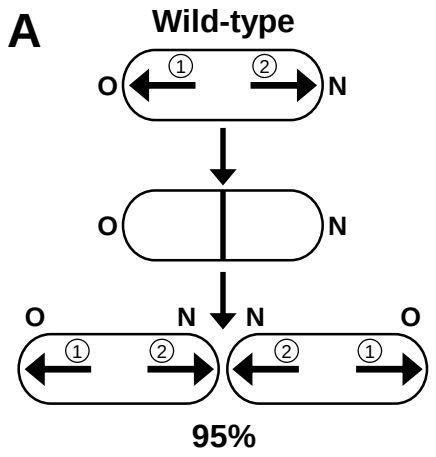

C Polarity of dominant end-containing cells

	gef1+ (n=39)	*gef1Δ* (n=74)
monopolar	3%	81%
NETO	97%	9%
precociously bipolar	0%	9%

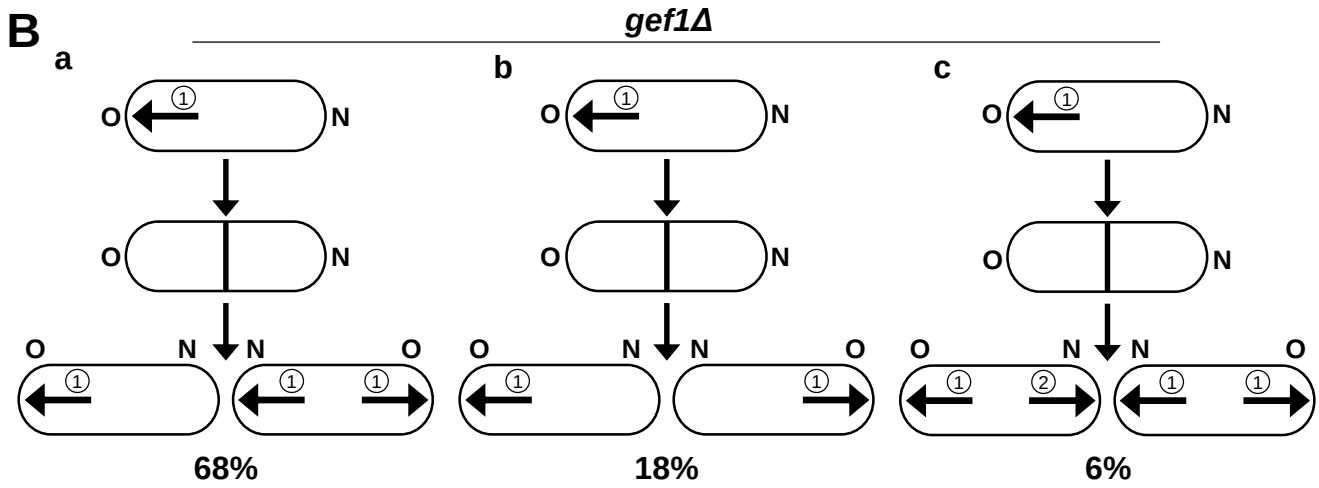

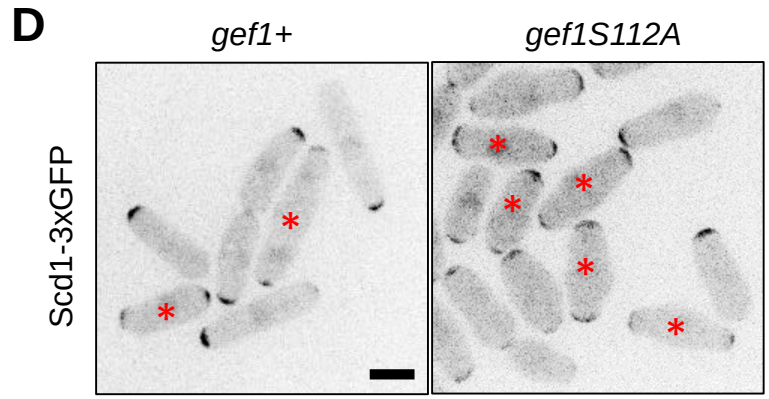

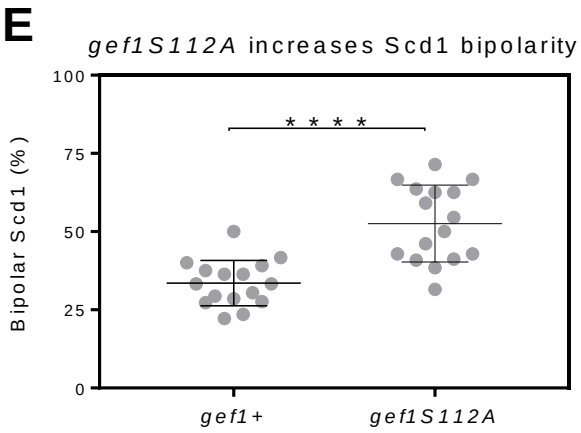

Figure 5

Figure 5: Gef1 promotes bipolar growth via new-end-take-off . (**A**) Wild-type cells predominately display old end growth followed by a delayed onset of new-end growth. **(B) i.** In *gef1Δ*, 68% of monopolar cells yield a monopolar cell from the end that grew in the previous generation and a bipolar cell from the end that failed to grow in the previous generation. **ii**.18% of monopolar cells yield two monopolar cells. **iii**. 6% of monopolar cells yield two monopolar cells. Circled numbers describe the order of growth. Arrows correspond to direction of growth. **(C)** Quantification of the fate of *gef1+* and *gef1Δ* cells with a dominant end. **(D)** Localization of Scd1-3xGFP to the cell poles in *gef1+* and *gef1S112A* cells. Asterisks indicate cells with bibolar Scd1-3xGFP localization. **(E)** Quantification of the percent of cells that exhibit bipolar Scd1-3xGFP localization at cell ends in the indicated genotypes (****, $p<0.0001$). Scale bar = 5µm.

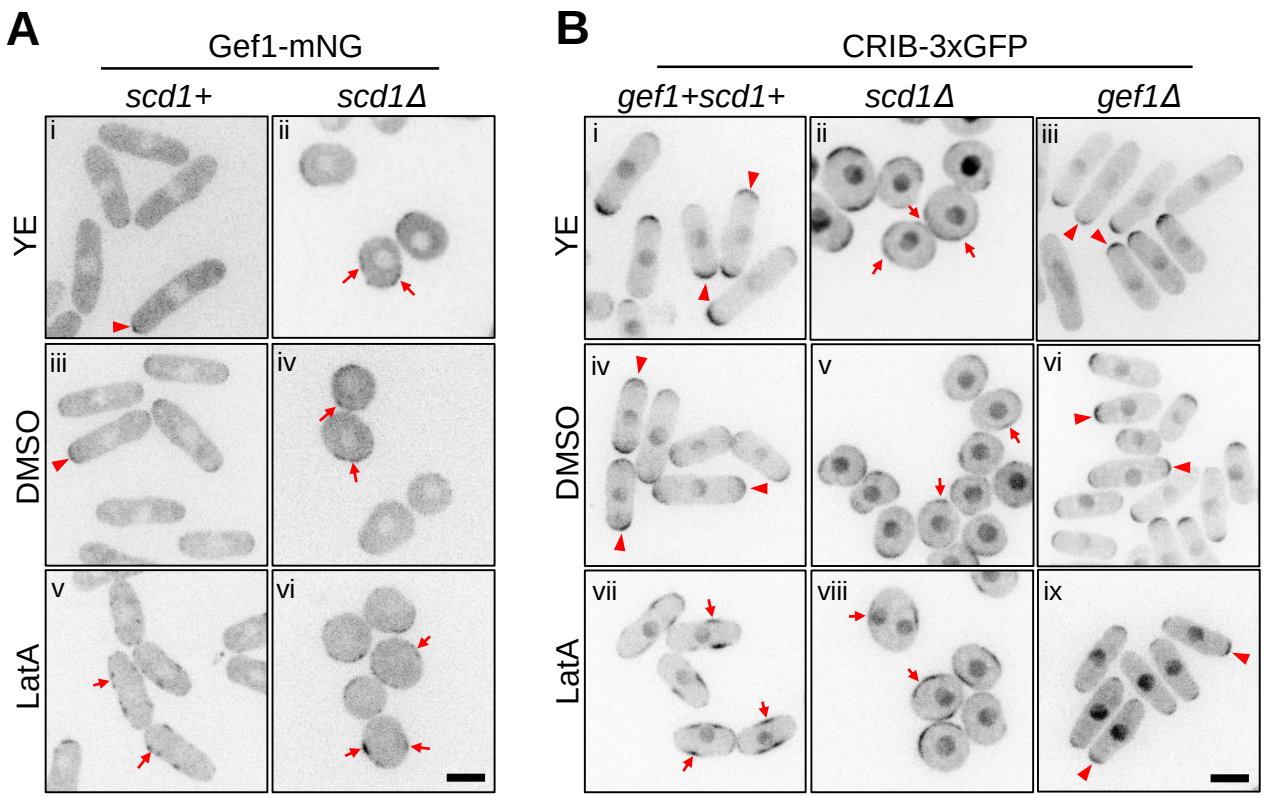

Figure 6: Scd1 and actin prevent ectopic Gef1 localization to promote polarized growth. (A) Gef1-mNG localization in *gef1+* and *gef1Δ* cells grown in yeast extract (YE, top panel) or treated with DMSO (middle panel) or 10µM LatA (bottom panel). **(B)** CRIB-3xGFP localization in *gef1+* and *gef1Δ* cells treated with DMSO (top panel) or 10µM LatA (bottom panel). Arrowheads indicate cells with CRIB-3xGFP or Gef1-mNG localized to regions of polarized growth. Arrows indicate cells with CRIB-3xGFP or Gef1-mNG localized to non-polarized regions on the cell cortex. All images are inverted max projections of the medial 4-7 cell slices. Scale bar = 5µm.

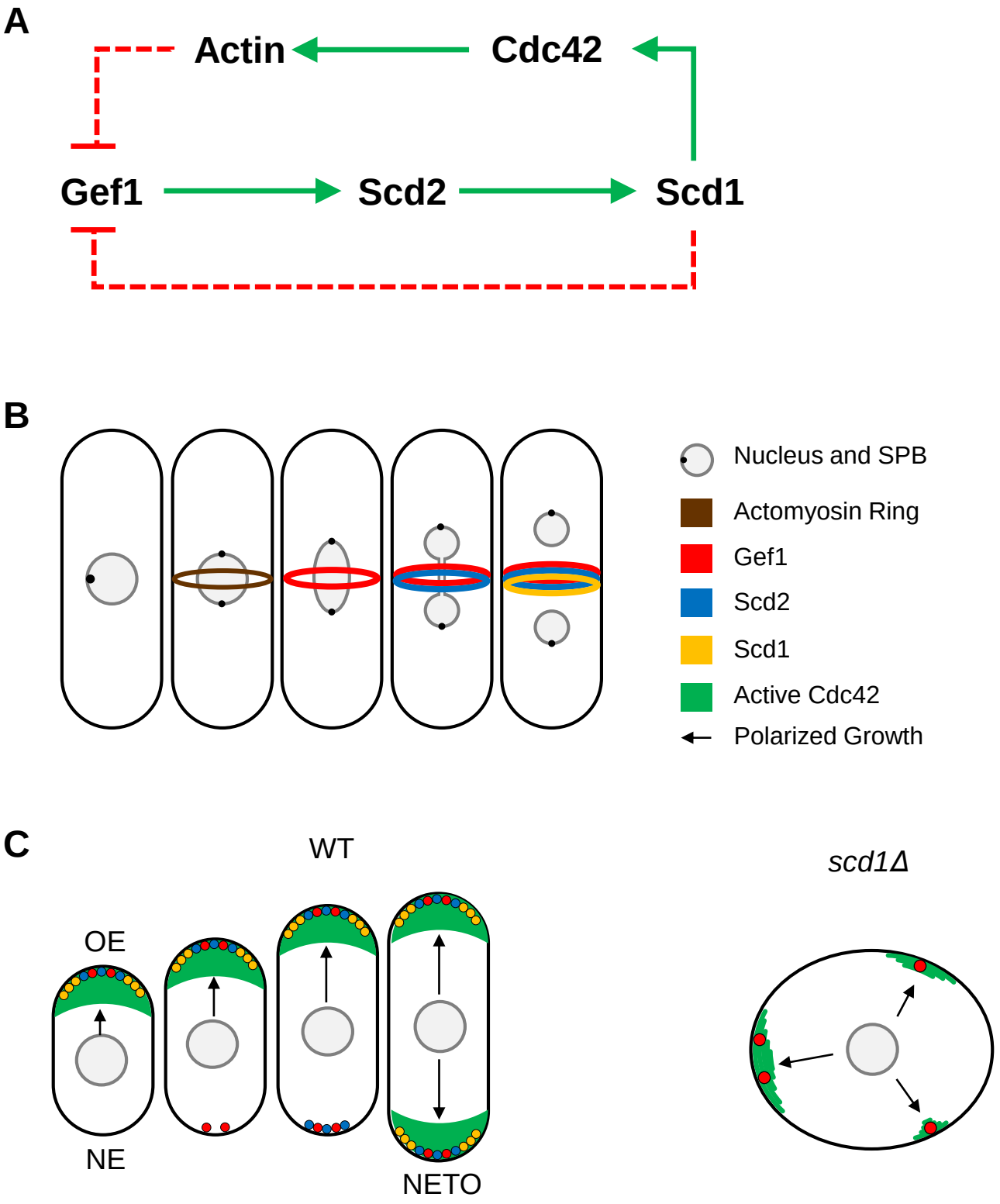
A
Actin
Cdc42
Gef1
Scd2
Scd1
B
Nucleus and SPB
Actomyosin Ring
Gef1
Scd2
Scd1
Active Cdc42
Polarized Growth
C
WT
scd1Δ
OE
NE
NETO

Figure 7

Figure 7: Model of the crosstalk between Gef1 and Scd1 that promotes polarized bipolar growth. (A) Diagram of the crosstalk pathway between Gef1 and Scd1. Solid arrows indicate an activating or promoting relationship in the direction of the arrow. Red terminating arrow indicates inactivation or removal of the protein at the arrows terminus. Dashed arrows indicate that the mechanism that regulates the proteins to which these arrows point is not yet resolved. **(B)** Schematic depicting the sequential localization of Gef1, Scd2, and Scd1 to the division site during cytokinesis. At the division site Gef1 localizes first and promotes Scd2 localization. Scd2 at the division site then recruits Scd1. **(C)** Schematic illustrating the crosstalk between Gef1 and Scd1 that promotes bipolar growth and regulates cell shape. In wild type (WT) cells, Gef1 localizes Scd2 to the new end, which in turn recruits Scd1 thus enabling NETO. In *scd1Δ* cells Gef1 localization is no longer restricted to the cell ends leading to ectopic Cdc42 activation and loss of polarity.